Renewable Energy 205 (2023) 200–221

Contents lists available at ScienceDirect

Renewable Energy

journal homepage: www.elsevier.com/locate/renene

Seismic dynamics of offshore wind turbine-seabed foundation: Insights from a numerical study

Kunpeng He, Jianhong Ye *

State Key Laboratory of Geomechanics and Geotechnical Engineering, Institute of Rock and Soil Mechanics, Chinese Academy of Sciences, Wuhan, 430071, China

ARTICLE INFO

Keywords:
Seismic dynamics
Offshore wind turbine
Seabed foundation
Pastor-Zienkiewicz-Mark III
Fluid-structure-seabed interaction
Monopile foundation
FssiCAS

ABSTRACT

In the past 10 years, the offshore wind energy harvest industry has developed rapidly worldwide. However, seismic waves would bring a great threat to the safety and stability of offshore wind turbines (OWTs). In this study, taking the marine geotechnics numerical software FssiCAS as the computational platform, adopting the generalized elastoplastic soil model Pastor-Zienkiewicz-Mark III (PZIII) to describe the complex mechanical behavior of seabed soil, the seismic dynamics, as well as the stability of a thin-walled monopile OWT with an equipped capacity of 1.5 MW and its seabed foundation are comprehensively investigated, by the way of finely modeling and meshing for the important components of the OWT, i.e., the blades, nacelle, and tower. The numerical results indicate that OWT and its seabed foundation strongly respond to the excitation of seismic waves, and there is intensive interaction between OWT and its seabed foundation. In the case of this study, the horizontal oscillation amplitude at the top of the turbine tower reaches 2m, the superficial seabed soil at the far field is liquefied with a depth of 3–4 m, and the liquefaction depth of the seabed soil surrounding the monopile reaches 5–6 m. Even so, the OWT involved in this study has no cumulative displacement, there is only vibration displacement. It is indicated that the OWT has good seismic stability. It is indicated by the comparative study that the complex mechanical behavior of seabed soil, the complex geometry and mass distribution of OWTs, and the consideration of the pore water in seabed foundations have a radical influence on the seismic dynamics of OWTs. The work presented could be a valuable reference for the evaluation of the seismic dynamics and stability of OWTs in the future.

1. Introduction

The wind energy harvest by offshore wind turbines (OWTs) is experiencing a rapid growth worldwide due to its advantages of the abundant reserves of wind energy, low environmental impact, saving land resources, the higher equipped capacity of a single unit, and cost efficiency. However, strong winds, extreme ocean waves and currents in typhoon weather could bring a great threat to the safety and stability of OWTs during their designed service period [1].

Besides the above-mentioned environmental loadings, some OWTs are built in zones with high earthquake intensity where strong earthquakes may occur, hence the seismic stability of OWT must be a critical design consideration. OWTs are a type of high-rise structure in offshore areas, leading to there is a great possibility of tilting and rotational failures due to the strong shaking in earthquake events. It is worth mentioning that two earthquakes occurred in 2021 (M_L = 5.0 with a source depth of 17 km) and 2020 (M_L = 3.1 with a source depth of 19 km) in the offshore area of Dafeng District, Yancheng city in Jiangsu Province, China, where more than 1000 OWTs with a total capacity of 9.45 GW have been built. It was reported that slight tilting has occurred for several monopiles of these OWTs, leading to a significant reduction of their service period. Besides, strong earthquakes with a magnitude greater than 7.0, even 9.0 often occur in the offshore zone of Japan, such as the 311 Tohoku earthquake in 2011. They have brought great threats to the safety and stability of offshore structures in Japan and have also become an important adverse factor hindering the development of the offshore wind industry in Japan. Therefore, it is of great engineering significance for the exploitation of offshore wind energy resources to study the seismic dynamics of OWTs and seabed foundations, and to establish a time domain evaluation method for the seismic stability of OWTs.

A number of works have been carried out on the seismic dynamic response of onshore wind turbines [2]. Due to the complex environmental loads, i.e., the extreme wind load, and ocean wave load, as well

* Corresponding author.
E-mail addresses: Yejianhongcas@gmail.com, Jhye@whrsm.ac.cn (J. Ye).

https://doi.org/10.1016/j.renene.2023.01.076
Received 12 November 2022; Received in revised form 14 January 2023; Accepted 19 January 2023
Available online 21 January 2023

as the possible seismic load, compared with onshore wind turbines, OWTs generally are less stable. Therefore, the research results of onshore wind turbines generally can't directly be applied to OWTs. The research methods on the seismic dynamics and stability of OWTs can be divided into two types: physical model tests and numerical simulations, respectively.

The physical model test can show the vibration responding and failure process of marine structures under seismic waves, which is an important technical means to study the seismic dynamics and performance of structures. At present, the seismic dynamics test for OWTs mainly includes two types: the 1 g shaking table test and the super-gravity centrifuge shaking table test. One advantage of the 1g shaking table test is that the cost is relatively low. Typical works in this field were conducted by Prowell [3] and Zheng et al. [4] etc. These works directly reflected the effect of seismic wave intensity on the dynamic response of OWTs. However, the similarity theory can't be strictly met in the 1g shaking table test. The stress and deformation in the test model are not similar to those in the prototype model. Wang et al. [5,6], Li et al. [7], Ji et al. [8], and Zhao et al. [9] studied the seismic dynamics of an OWT adopting centrifuge shaking table test. The shaking table test in super-gravity centrifuge devices overcomes the problem that the similarity theory can't be satisfied in the 1g test. Furthermore, the size of the physical model is small and the model preparation is relatively laborsaving.

The centrifugal model test indeed is an effective technique to study the seismic dynamics of OWTs. However, to deal with complex boundary conditions and avoid the influence of the mass of sensors on the dynamics of turbine blades, numerical modeling is widely used as an alternative way to handle the problem. Early studies generally didn't consider the interaction between the monopile and seabed soil but fixed the monopile of OWTs on seafloor which was treated as a rigid body. Typical works on this aspect were conducted by Gao et al. [10] and Guanche et al. [11]. However, the deformation of porous seabed foundation and its internal seepage would significantly change the natural frequency and the dynamic response characteristics of an OWT system. Yang et al. [12,13], and Zuo et al. [14] showed that a seabed foundation with elastoplastic deformation had a significant impact on the displacement at the top of the tower of OWTs, as well as the bending moment in the tower at the mudline.

Some scholars proposed to use of mathematical methods to describe the effect of seabed soil on the monopile of OWTs. Typical methods included the p-*y* curve method [15,16], the point stiffness matrix method for pile foundation [17], etc. Taddei et al. [18], Kathe and Kaynia [19], and Ko [20] studied the influence of shear modulus, elastic modulus, and damping of foundation soil and other parameters on the natural frequency of an OWT adopting the nonlinear spring elements to simulate the reaction force of foundation soil to the pile foundation. Abhinav and Saha [21], and Zuo et al. [22] studied the effect of pile-soil interaction on the seismic dynamics of OWTs. They found that the natural vibration frequency of the tower of OWTs was significantly reduced, and the dynamic response of the blades and tower of OWTs was significantly affected if the pile-soil interaction was considered. For the p-*y* curve method to deal with the pile-soil interaction, although the horizontal load on the monopile of OWTs is considered, the dynamic response of seabed foundation is ignored. Furthermore, a great deviation will arise if seabed foundation is simplified into a viscoelastic solid in the seismic stability analysis for OWTs [23].

To reveal the interaction mechanism between pile foundation and seabed soil, and consider the influence of the deformation and softening of seabed soil on the bearing capacity of pile foundation of OWTs, Wang et al. [24], Wang et al. [25], Ali et al. [26] studied the seismic dynamics of an OWT utilizing the 3D finite element method by establishing the whole geometrical model of the OWT and its seabed foundation, in which the interaction between pile foundation and seabed soil was described by the contact elements or the binding boundary method. Prendergast et al. [27], and Ma et al. [28] studied the change of the lateral bearing capacity of seabed foundation, and the overall seismic performance of an OWT after scour, in which the local scour pit around the pile of OWT was finely characterized by finite element meshes. However, the turbine blades, nacelle, etc. were not modeled in these above-mentioned works. Meng et al. [29] and Cui et al. [30,31] provided a novel approach to describe the dynamic interaction system of a large-diameter floating pipe pile and surrounding soils and investigated the soil-pile coupled vibration under dynamic loads. Alternately, the turbine blades, nacelle, etc. were simplified into a vertical concentrated force applied to the top of turbine towers in most previous literature. It has been indicated by Ref. [32] that there was very significant deformation in the blades in the analysis of the seismic dynamics for the OWTs with megawatt capacity. The neglect of the complex geometry of turbine blades and nacelle will lead to a great error in the seismic dynamics analysis.

Yan et al. [33] studied the effect of different foundation forms on the seismic performance of an OWT by utilizing several hundreds of thousands of structural elements, but the turbine blades were also not modeled. Mardfekri [34] and Anastasopoulos [35] adopted the centralized mass elements to simulate the hub and blades, and Xi et al. [36], Mo et al. [37] adopted the beam and shell elements to simulate the blades and monopile foundation to study the seismic dynamics of OWTs. In this kind of work, although the turbine blades were considered, and the whole finite element model for OWTs was established, the complex mass distribution of turbine blades could not be considered. It was indicated by previous works [38] that the adoption of beam elements would arise great errors for OWTs since the diameter of the tower and monopile were so large, and the change rate of the blade section was also significant. As it is well known, the beam element is more applicable for slender structures, however, OWTs with blades and nacelle are not slender structures. Since the great difficulty of the mesh generation for turbine blades, there are few studies available so far in which OWTs and seabed foundations are discretized by utilizing finite element entity elements.

In some studies, the governing equations for fluid dynamics and soil-structure dynamics were coupled in an iterative way, to establish numerical models for the seawater-OWT-seabed foundation coupling interaction, which had been widely used to study the ocean wave-induced dynamic response of OWTs and their seabed foundation. The typical works were performed by Zhang et al. [39], Lin et al. [40], and Wang et al. [41]. However, the seismic loads, as well as the complex geometry and mass distribution of turbine blades couldn't be taken into account in those previous works. What's more, the complex mechanical behavior of seabed soil also couldn't be described in them. The seabed soil only can be treated as linear poroelastic materials. It is commonly known that the real seabed foundation soil is never linear elastic, but elastoplastic. Therefore, the above-mentioned numerical models can't be applicable in practical engineering. Yang et al. [42], and Asareh et al. [43] also developed a module to analyze the seismic dynamics of OWTs based on the Open-source code FAST. However, the effect of the complex mechanical behavior of seabed soil still couldn't be considered in their module.

Jeng et al. [44] and Ye et al. [45] developed an integrated numerical model FSSI-CAS 2D/3D for the problem of ocean/seismic wave-structure-seabed interaction. Lately, It evolved into the software FssiCAS (Fluid-Structure-Seabed Interaction, Chinese Academy of Sciences), and is currently available at http://www.fssi.ac.cn/download.html. The software FssiCAS not only can consider the seismic or hydrodynamic loads but also can implement the coupled interaction between seawater, marine structures, and seabed foundation. Furthermore, there are a series of elastoplastic soil models available to the users. FssiCAS has been successfully applied to study the dynamics of offshore breakwaters under ocean waves [46] or seismic waves [47]. However, FssiCAS has not been applied to study the seismic dynamics of OWTs with complex geometry and large diameter.

In this study, taking the software FssiCAS as the computational

Table 1
Parameters of the OWT with a capacity of 1.5 MW

Component	Property	Value	Property	Value
Blades	Roto Diameter	77.00 m	Tensile modulus	140.00 GPa
	Length	33.30 m	Shear modulus	4.38 GPa
	Density	1570 kg/m3	Poisson's ratio	0.17
Generator system	Hub Diameter	3.00 m	Nacelle mass	40.00 t
	Hub mass	8.00 t		
Tower	Length	65.00 m	Density	8500.00 kg/m3
	Bottom diameter	3.50 m	Elastic modulus	210.00 GPa
	Top diameter	3.00 m	Shear modulus	80.80 GPa
	Wall thickness	0.05 m	Poisson's ratio	0.30
Monopile	Length	47.00 m	Density	7850.00 kg/m3
	Length buried in soil	30.00 m	Elastic modulus	210.00 GPa
	Diameter	5.00 m	Shear modulus	80.80 GPa
	Wall thickness	0.05 m	Poisson's ratio	0.30

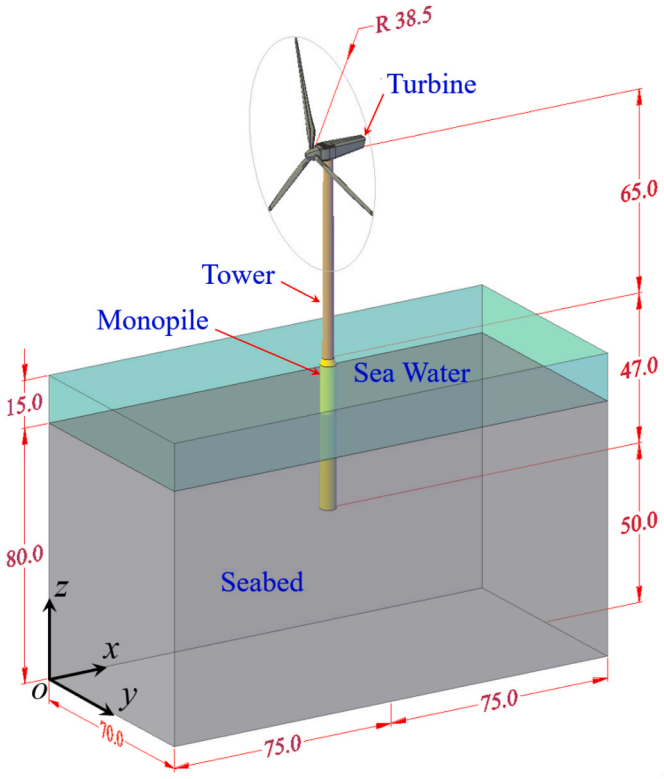

Fig. 1. Schematic diagram of an OWT with a monopile installed in a seabed foundation (Unit: m).

platform, taking a thin-walled monopipe OWT with an equipped capacity of 1.5 MW as the object, and adopting the generalized elastoplastic soil model Pastor-Zienkiewicz-Mark III (PZIII) to describe the complex mechanical behavior of seabed soil, the seismic dynamics, as well as the stability of the monopile OWT and its seabed foundation are comprehensively investigated, by the way of finely modeling and meshing for the important components of the OWT, i.e., the blades, nacelle, and tower. Furthermore, several comparative analyses are

Table 2
Essential parameters of seabed foundation soil.

Volumetric modulus E_s (MPa)	Elastic modulus E (MPa)	Poisson's ratio ν	Permeability k (m/s)	Void ratio e
2.92	1.56	0.33	0.0001	0.65

Table 3
Constitutive model parameters of PZIII for the seabed foundation.

Parameter	Value	Parameter	Value	Parameter	Value
K_{evo} (kPa)	2000	$\propto_f$	0.45	H_0	750
G_{eso} (kPa)	2600	$\propto_g$	0.45	H_{U0} (kPa)	40000
$P_0^{'}$ (kPa)	4	β_0	4.2	γ_u	2.0
M_g	1.32	β_1	0.2	γ_{DM}	4.0
M_f	1.3				

Noted: $\boldsymbol{K_{evo}}$ is bulk modulus of the soil, $\boldsymbol{G_{eso}}$ is three times the shear modulus of the soil, $\boldsymbol{P_0^{'}}$ is reference mean confining stress at which the moduli are evaluated, $\boldsymbol{M_g}$ is the slope of the critical state line for determination of loading vector, $\boldsymbol{M_f}$ is the slope of the critical state line for determination of plastic strain vector, $\propto_f$ is parameter which determines relationship of dilatancy with stress ratio for plastic strain vector, $\propto_g$ is parameter which determines relationship of dilatancy with stress ratio for loading vector, $\boldsymbol{\beta_0}$ is constant for shear hardening, $\boldsymbol{\beta_1}$ is constant for shear hardening, $\boldsymbol{H_0}$ is constant for the loading plastic modulus, $\boldsymbol{H_{U0}}$ is constant for the unloading plastic modulus, $\boldsymbol{\gamma_u}$ is the rate of change of unloading slope, $\boldsymbol{\gamma_{DM}}$ is the rate of change of the initial reloading slope.

conducted to explore the effect of the complex mechanical behavior of seabed soil, the complex geometry of blades and nacelle, the initial hydrostatic pressure, and the pore water on the seismic dynamics of the OWT. It is worth mentioning that the OWT involved in this study is only 1.5 MW, the capacity of some existing OWTs has exceeded 10 MW. Nevertheless, this study aims to provide an analysis method for such problems, which should also be applied to ultra-large OWTs. One more thing that needs to be noted is that, since the possibility of extreme ocean waves in the sea area where an OWT is located is extremely small when a strong earthquake occurs, the simultaneous effect of ocean waves on the OWT is not considered in this study.

2. Numerical implementation

2.1. Geometric model of OWT-seabed foundation

A thin-walled steel monopile OWT with a capacity of 1.5 MW is selected as the research object in this study, and the main parameters of the OWT are listed in Table 1. The monopile foundation is a large-diameter thin-walled hollow steel pipe with a diameter of 5.0 m, and a wall thickness of 5 cm. The monopile foundation is driven into the seabed foundation with a depth of 30 m. The lateral friction resistance provided by the seabed soil inside and outside the hollow steel monopile together provides the vertical bearing capacity to support the OWT. The 3D geometric model of the OWT and its seabed foundation established in this study is shown in Fig. 1. The coordinate origin point '*O*' is set at a vertex on the left lateral side of the computational domain. The seabed foundation is 150 m long, 70 m wide and 80 m thick.

In the marine environment, seabed foundations are generally the newly and rapidly deposited soil layers in the Quaternary. They are typically characterized by softness and low bearing capacity. Under cyclic loading, they are highly susceptible to become softened or liquefied. The basic parameters of the seabed foundation are listed in Table 2. In fact, the mechanical behavior of seabed soils generally is extremely complex, and advanced elastoplastic soil models must be used to credibly describe their mechanical behavior. In this study, the generalized elastoplastic soil model Pastor-Zienkiewicz-Mark III (PZIII)

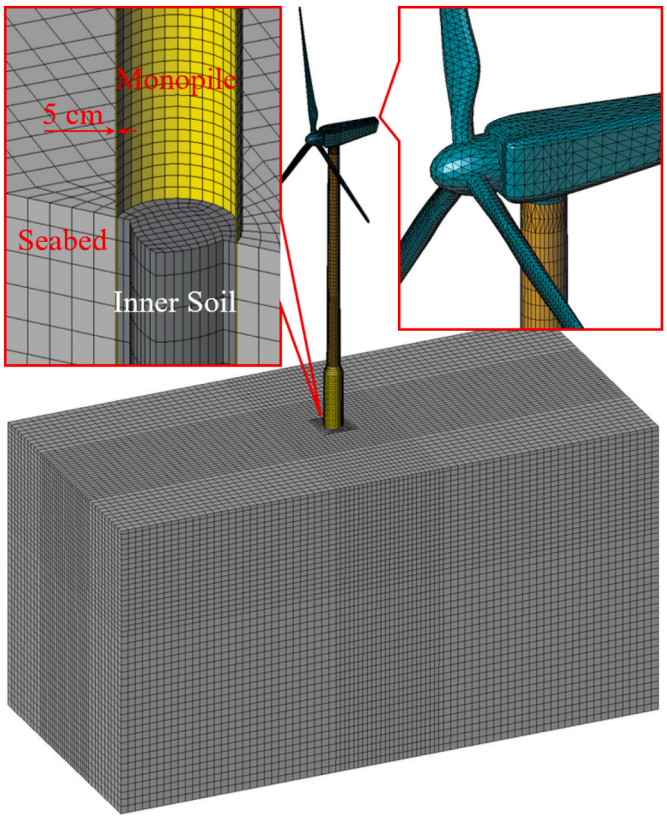

Fig. 2. Mesh generation for the OWT and its seabed foundation.

proposed by Pastor et al. [48], is utilized to describe the dynamic behavior of the seabed foundation. The reliability of the PZIII soil model has been demonstrated by a series of monotonic and cyclic loading tests, including the centrifuge tests in the famous VELACS project [44]. Additionally, the PZIII model has been successfully applied in the study of the dynamic response of marine structures such as breakwaters [46], submarine pipelines [49], and OWTs [59], etc. The soil parameters of the PZIII model for the seabed foundation used in this study are listed in Table 3, which were calibrated and used by Zienkiewicz et al. [50] when they participated in the VELACS project.

2.2. Mesh generation

As shown in Fig. 2, this study overcomes the difficulties of modeling and meshing the complex marine structures, the OWT and seabed foundation are finely discretized utilizing finite elements, considering the real geometry of the turbine blades, nacelle, and the thin-walled steel monopipe. Among them, tetrahedron elements are used for the turbine blades and nacelle, and hexahedron elements for the turbine towers and seabed foundation. The total number of elements in the whole computational domain is about 200,000, and the total degree of freedom is about 900,000. The element size in the turbine blades is about 0.8 m, and the minimum element size in the seabed foundation surrounding the monopile is about 0.5 m. Compared to the simplified beam elements, the adoption of entity elements allows for a more accurate description of the complex geometric shape of the OWTs, as well as the corresponding mass distribution. Furthermore, the bending moment distribution in the wind turbine tower also could be reliably estimated through some integration algorithms on the entity elements in the tower.

Currently, there are three approaches that are widely used to deal with the pile-soil interaction: (1) p-*y* curve method, (2) interface contact algorithm, and (3) common nodes method, respectively. It has been demonstrated by previous studies [51] that the p-*y* curve method was difficult to accurately describe the complex mechanical interaction between a loose seabed soil and a monopile, and this method would significantly overestimate the horizontal bearing capacity of seabed soil. The contact algorithm is to deal with the pile-soil interaction through the use of a penalty function in the finite element solving process, which is able to describe the slip and separation phenomena between soil and structures. Theoretically, the contact algorithm is much more reliable, but the computational consumption would increase significantly, and the contact parameters are not easily and appropriately determined. Besides, convergence is also a great challenge. For the cases where the pile-soil separation and tangential relative slip are not easy to occur, the method of common nodes not only can ensure the reliability of the results but also has high computational efficiency. Since the software FssiCAS is currently unable to implement the contact algorithm (this feature is expected to be available next year), the pile-soil interaction will be handled by adopting the common nodes method in this study.

2.3. Boundary conditions

The applied boundary conditions applied in the computation are as follows.

(1) Periodic or laminar boundaries are applied on the front and back sides of the seabed foundation, i.e., $u_x|_{y=0} = u_x|_{y=70}$, $u_y|_{y=0} = u_y|_{y=70}$, $u_z|_{y=0} = u_z|_{y=70}$, $p|_{y=0} = p|_{y=70}$.
(2) Periodic or laminar boundaries are applied on the left and right sides of the seabed foundation, i.e., $u_x|_{x=0} = u_x|_{x=150}$, $u_y|_{x=0} = u_y|_{x=150}$, $u_z|_{x=0} = u_z|_{x=150}$, $p|_{x=0} = p|_{x=150}$.
(3) The bottom of the seabed foundation is fixed, i.e., $u_x|_{z=0} = 0$, $u_y|_{z=0} = 0, u_z|_{z=0} = 0$. Additionally, the seismic wave is input on this fixed bottom.
(4) Hydrostatic water pressure is applied on the outer surfaces of the monopile and the seabed foundation in the range of $80\ \text{m} \le z \le 95\ \text{m}$. It is well known that, an extreme ocean wave could cause excessive displacement of OWTs, softening and liquefaction of seabed foundation. Neglecting the ocean wave in this modelling will lead to an overestimation of the safety factor of the OWT, which is detrimental to the stability of the OWT. However, the possibility of an extreme ocean wave in the sea area where an OWT is located is extremely small when a strong earthquake is occurring. Therefore, the simultaneous effect of ocean wave with seismic wave on the OWT is not considered in this study. Accordingly, there is no hydrodynamic pressure on the monopile and seabed foundation.

Regardless of physical model tests or numerical simulations, the reflection of seismic waves at the model boundary is a problem that requires attention. Usually, the effect of seismic wave reflection can be weakened to some extent by using a stacked laminar shear model box in physical model tests. In the numerical simulation, there are three methods that could avoid and weaken the effect of seismic wave reflection: (1) Lateral sides of the computational domain all are fixed, but the size of the computational domain could be appropriately enlarged. This method is simple to operate, but it will increase the computation workload. (2) Absorbing boundaries are utilized. This method works quite well for the absorption of reflected waves, but the theory is relatively complex and the computation workload is also considerable. It is generally used for the absorption of high-frequency components, and instantaneous bursting shock waves on boundaries. (3) For the computational domain with symmetry, periodic/laminar boundaries can be used to eliminate the reflection of seismic waves. This method is simple in operation and the computation workload is reasonable, but the computational domain must be symmetric. In this study, the seabed foundation is symmetric along the two planes of $x =$

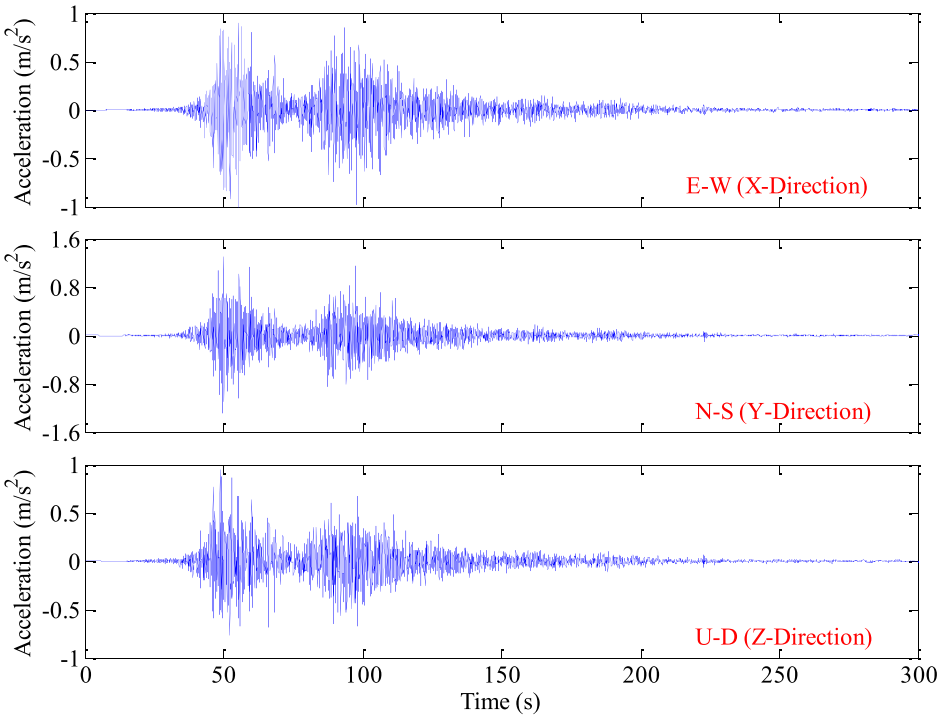

Fig. 3. Input seismic wave recorded at the downhole station MYGH03 during the 2011 Tohoku 311 earthquake in Japan.

Table 4
List of cases involved in this study.

Case No.	Case 1	Case 2	Case 3
Schematic diagram	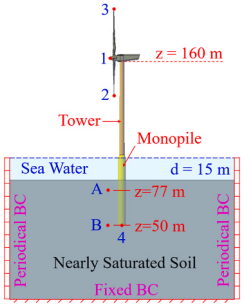	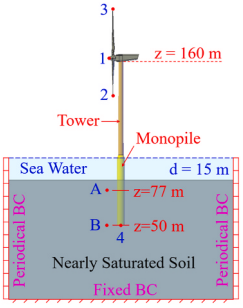	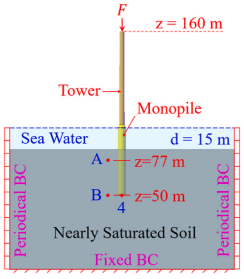
Shape of OWT	Real geometric shape	Real geometric shape	Equivalent loading method
Soil model	PZIII	Elastic	PZIII
Water depth	d = 15 m	d = 15 m	d = 15 m

Case No.	Case 4	Case 5
Schematic diagram	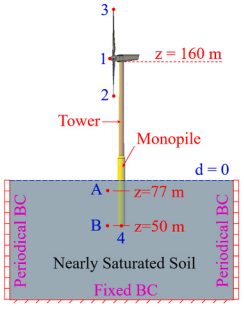	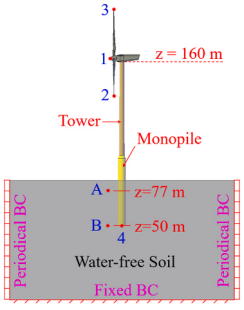
Shape of OWT	Real geometric shape	Real geometric shape
Soil model	PZIII	PZIII
Water depth	d = 0	Water-free

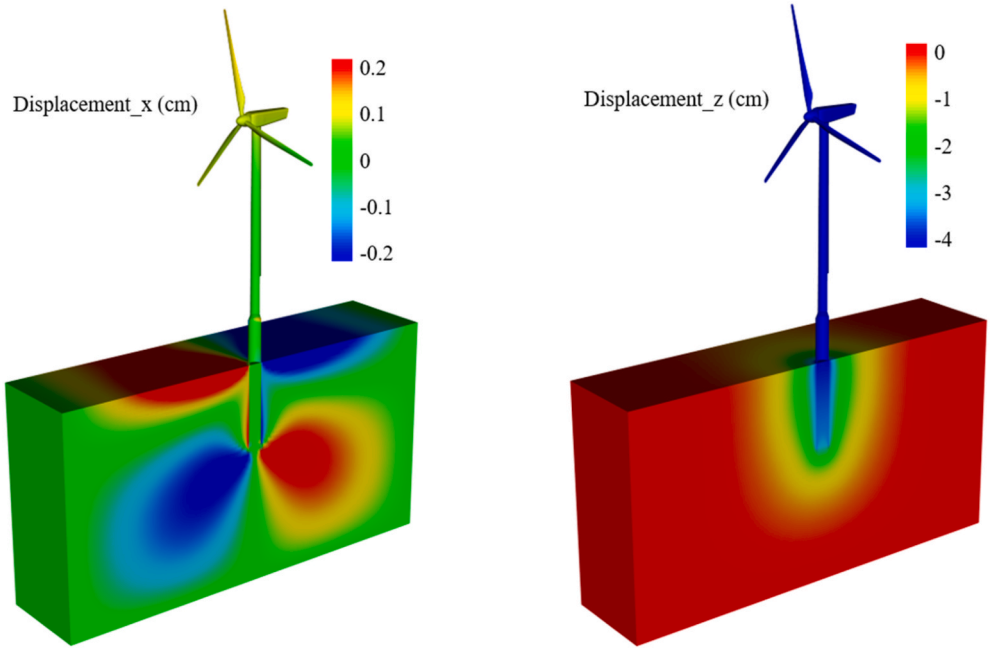

Fig. 4. Displacement distribution of the OWT and seabed foundation at the initial state.

75 m and $y = 35$ m, respectively. Therefore, the unfavorable effect of reflected waves on the seismic dynamics of the OWT and seabed foundation can be eliminated by utilizing the periodic/laminar boundaries.

2.4. Excited seismic wave

The study conducted here aims to understand the general mechanism for the seismic dynamics of OWTs and seabed foundations, rather than a real case study. Therefore, there is no mandatory requirement for the input seismic wave, especially the requirement on the location where the input seismic waves are recorded. In this study, the real seismic waves recorded in the 2011 Tohoku 311 great earthquake in Japan are selected as the input excitation seismic wave. This seismic wave was recorded by the observatory MYGH03 (141.6412E, 38.9178N), located near the Pacific coast, and 154 km from the epicenter. It has been used as input shaking by several researchers [47,52]. The time histories of the acceleration of the input seismic wave in the E-W (x-direction), N–S (y-direction), and U-D (z-direction) directions are shown in Fig. 3. The input excitation seismic wave presented the first peak at the moment $t =$ 50 s and the second peak at $t = 100$ s, and the peak acceleration is about 0.1 g.

In this study, there are a total of 5 cases are set up, as shown in Table 4. Case 1 is the standard case, which takes into account the complex geometry and mass distribution of the OWT, as well as the complex mechanical behavior of the sea foundation. Case 2 to Case 5 are the comparative cases, which are used to explore the effects of the complex mechanical behavior of the seabed soil, the complex geometry of the OWT, the initial hydrostatic pressure, and the pore water, respectively.

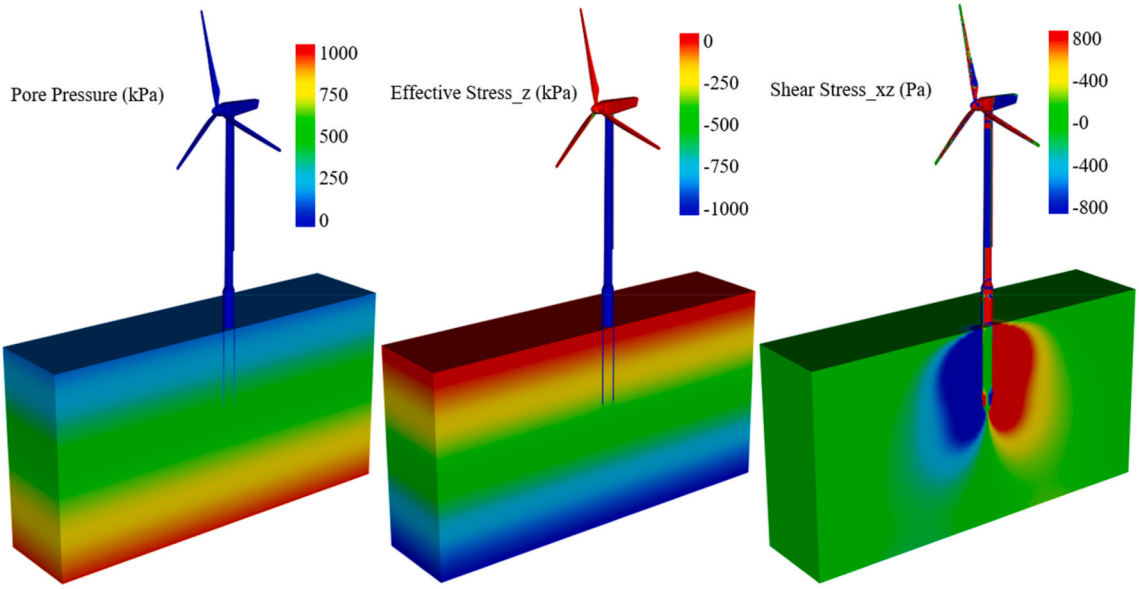

Fig. 5. Distribution of effective stress and shear stress at the initial state.

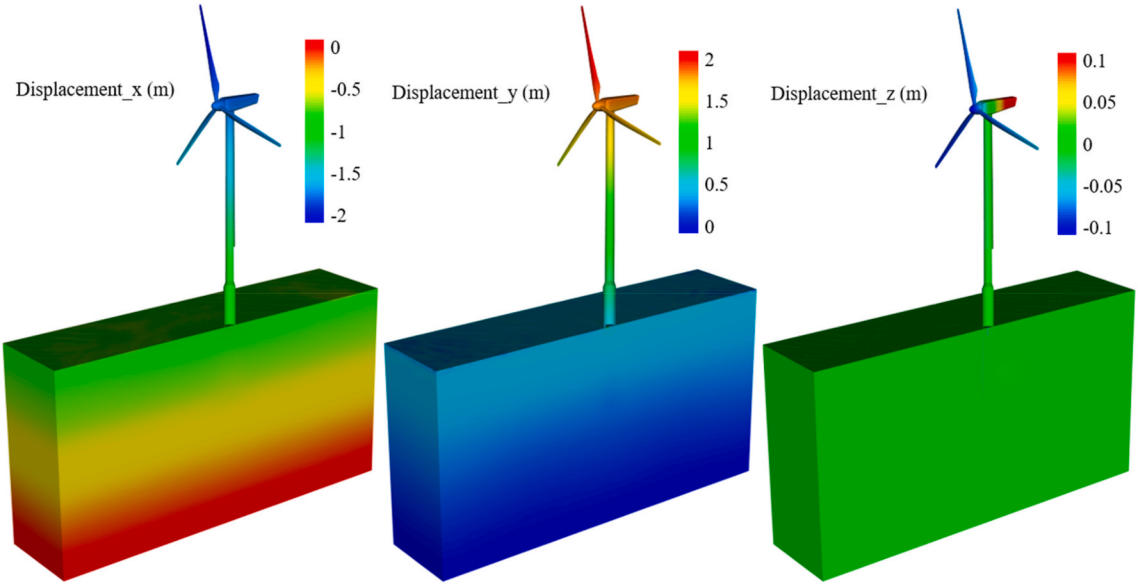

Fig. 6. Sectional view of the displacement distribution under seismic excitation at $t = 100$ s ($y = 35$ m).

3. Results and discussion

3.1. Initial state

The seabed foundation must have been in a state of equilibrium before the OWT was built. After the construction of the OWT and before the earthquake arrived, there certainly was subsidence for the OWT due to its dead weight, and a new equilibrium state for the OWT and its seabed foundation was reached. This new equilibrium state should be taken as the initial state for the subsequent dynamic analysis.

The settlement of the OWT and the deformation of the seabed foundation subjected to the dead weight of the OWT are shown in Fig. 4. It can be seen that the vertical settlement of the OWT is about 4 cm, and the horizontal displacement is only 0.1 cm. The turbine tower is in vertical position. It is indicated that the mass distribution of the blades and nacelle is reasonable, and the center of gravity of the upper structures is located on the central axis of the tower. As the interaction between the monopile and seabed soil is handled by the way of the common nodes in this study, when the vertical settlement of the monopile occurs, the coordinated deformation correspondingly is produced in the surrounding seabed soil.

Pore pressure and effective stress distribution in the OWT and its seabed foundation at the initial state are shown in Fig. 5. It can be seen that the pore pressure and vertical effective stress inside the seabed foundation are laminarly distributed after the construction of the OWT. Due to the settlement of the OWT relative to the seabed foundation, the maximum shear stress σ_{xz}' in the surrounding seabed soil of the monopile is only about 1 kPa.

3.2. Dynamic response

In the following, the seismic dynamics of the OWT and its seabed

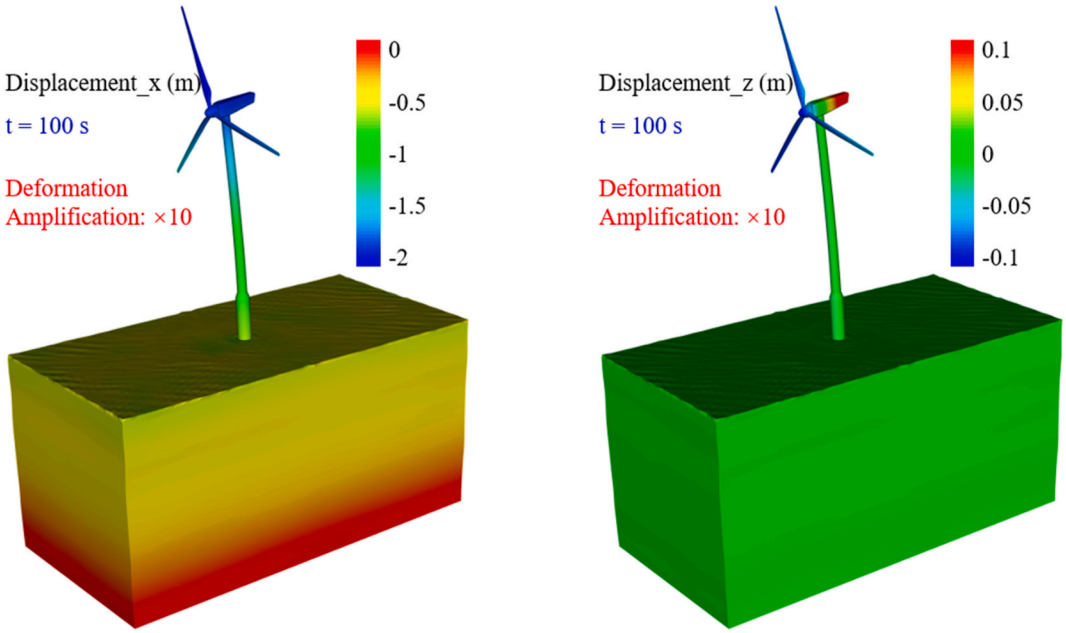

Fig. 7. Displacement distribution of the OWT and seabed foundation at $t = 100$s after the deformation is amplified by 10 times.

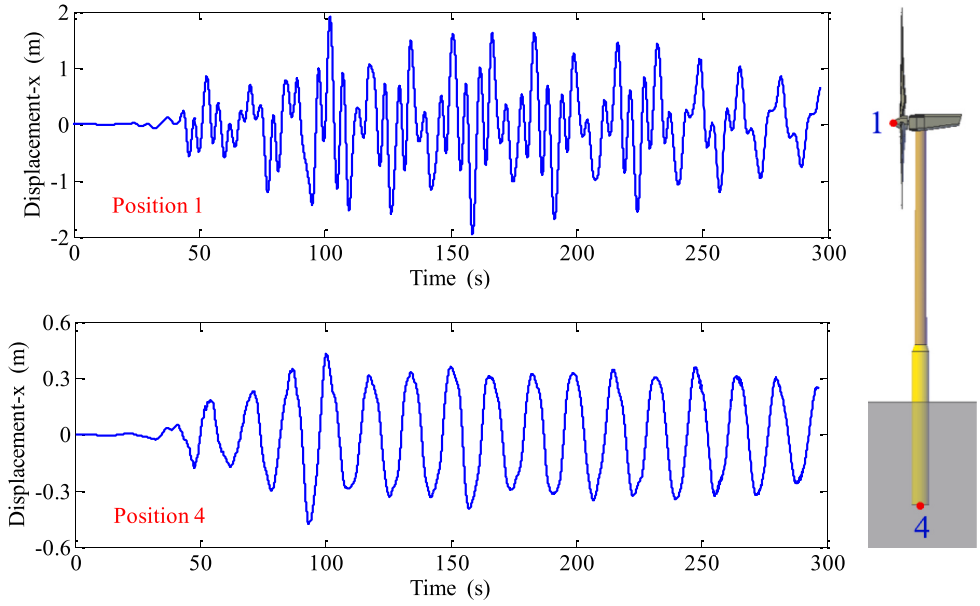

Fig. 8. Time histories of horizontal displacement at Position 1 at the center of blades, and Position 4 on the bottom of the monopile.

foundation, such as the displacement and bending moment of the monopile, the pore pressure and effective stress inside the seabed, and the liquefaction zone are analyzed, then the stability of the OWT is evaluated.

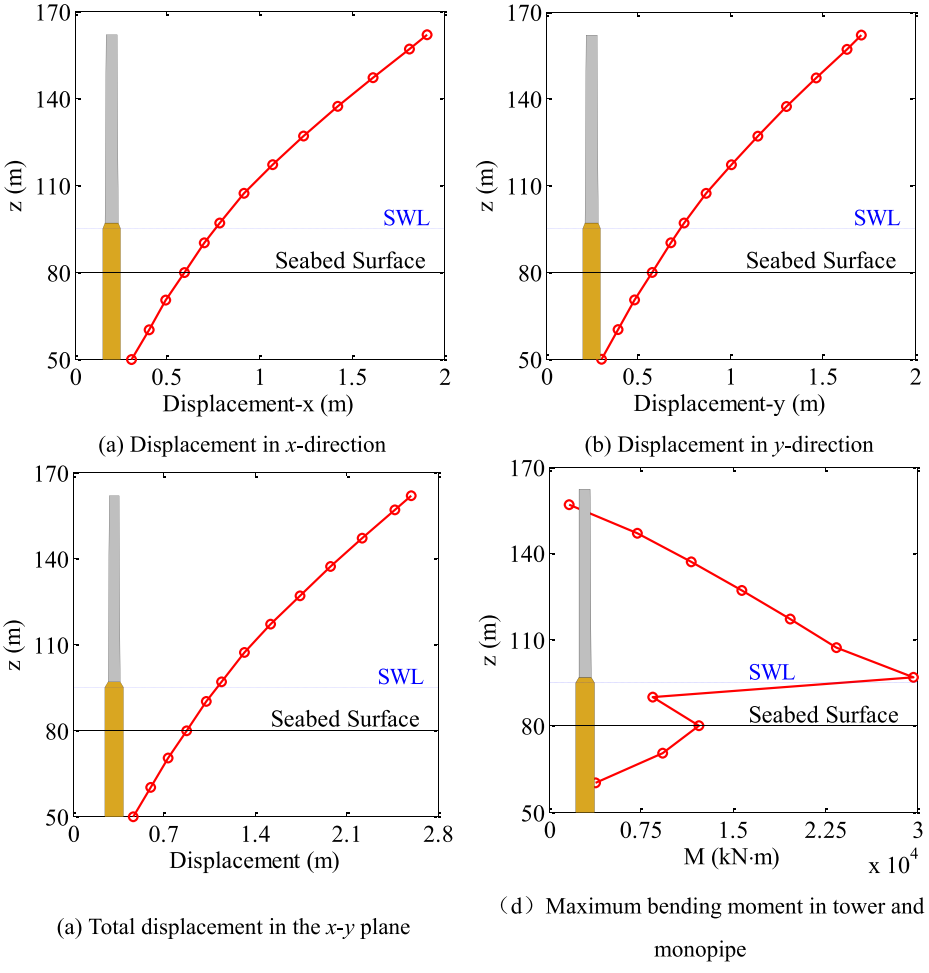

Fig. 9. Horizontal displacement and bending moment along the height of the OWT at the moment when they reach the peaks.

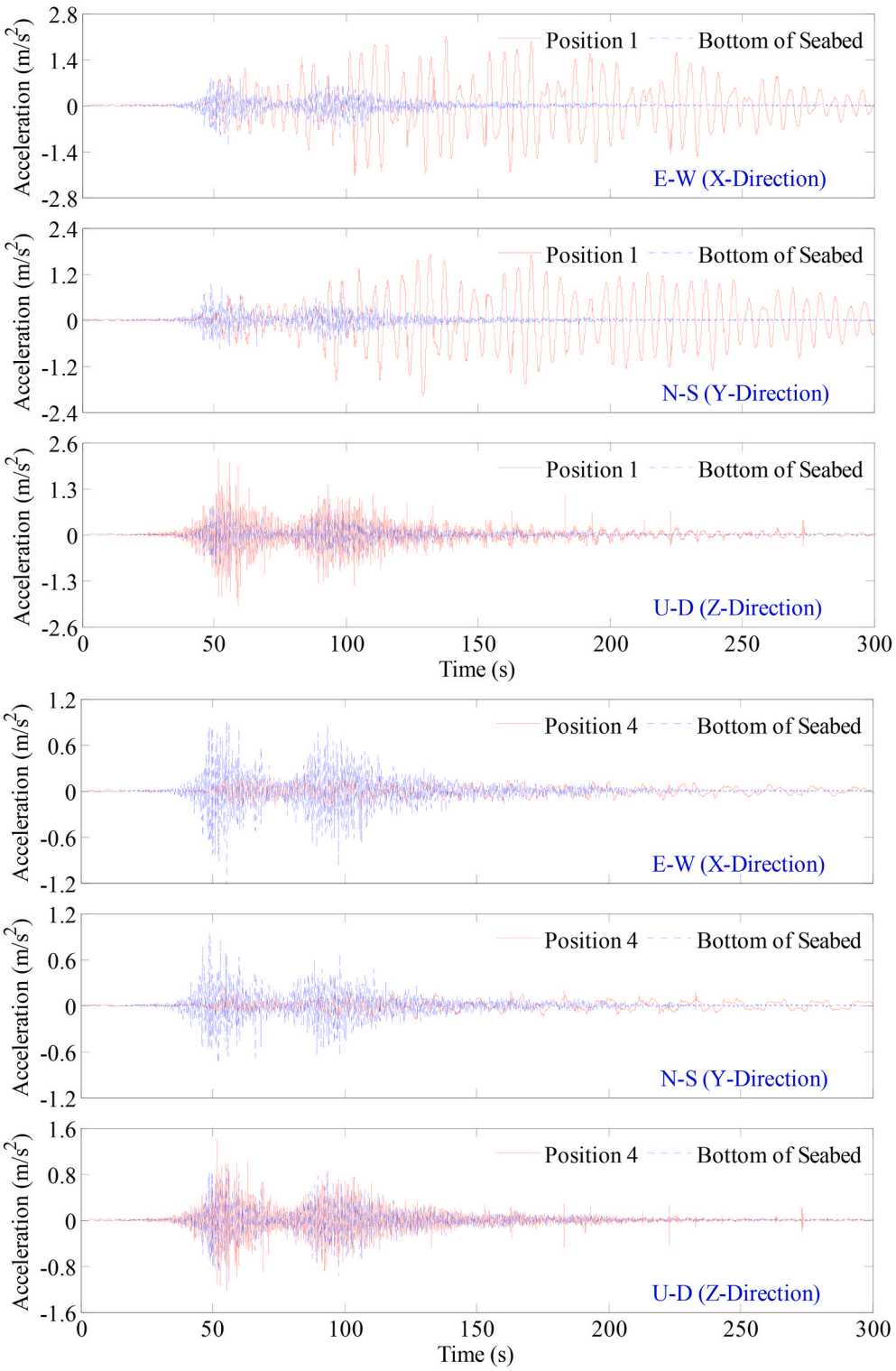

Fig. 10. Comparison of the accelerations recorded at Position 1, and Position 4 with the input seismic wave.

3.2.1. Displacement and bending moment

The displacement distribution in the OWT and its seabed foundation at $t = 100$ s is shown in Fig. 6. It can be seen that the displacement at the bottom of the seabed foundation is zero, and the horizontal displacement (x-direction and y-direction) is positively correlated with the height at which it is located. The maximum horizontal displacement is about 2 m, appearing at the top of the blades. The vertical displacement of the seabed foundation is basically zero, the vertical displacement of the blades is about −0.1 m, and the vertical displacement of the nacelle is about 0.1 m. This result indicates that the OWT vibrates strongly and tilts to the lateral side with an amplitude of about 2 m under seismic action. In addition, it can also be seen in Fig. 6 that the horizontal displacements of the seabed foundation are all distributed in layers. It indicates that a horizontal shear motion occurs in the seabed foundation under the constraint of the applied periodic boundary conditions, achieving an effect similar to that of a laminar shear box in physical

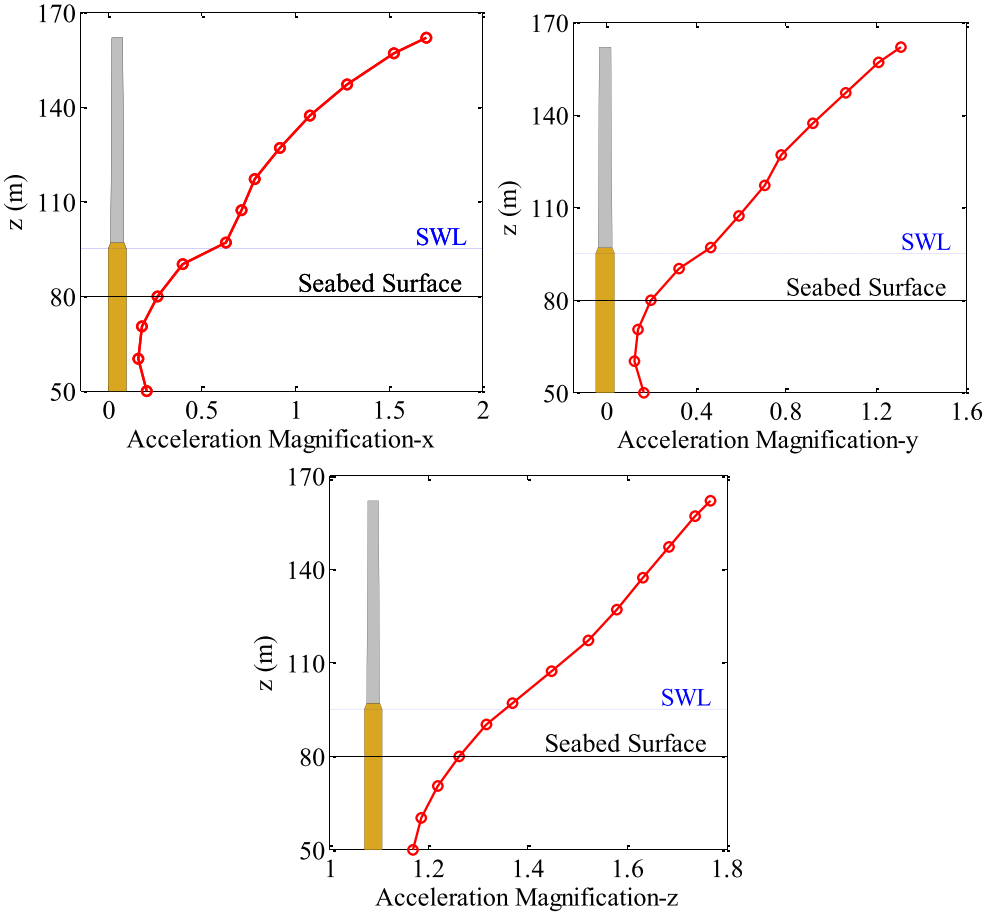

Fig. 11. Peak acceleration magnification along the tower and monopile of the OWT relative to the input seismic wave.

model tests.

Fig. 7 shows the displacement distribution and the corresponding deformation of the OWT and its seabed foundation at $t = 100$s after the deformation is magnified by 10 times. In this way, the displacing characteristics of the OWT and its seabed deformation can be observed more clearly. The OWT tilts significantly to the left, and a horizontal laminar shear deformation also occurs in the seabed foundation to the left at this moment.

Fig. 8 shows the time histories of displacement at Position 1 (at the center of the blades) and monitoring Position 4 (on the bottom of the monopile). It can be seen that the OWT vibrates strongly with a large amplitude, but there is no residual displacement occurs. The maximum vibrating amplitude at Position 1 at the top of the OWT is 1.9 m in the *x*-direction. The corresponding tilting angle of the tower is about 1°, which has seriously exceeded the requirement for the verticality of the tower in many OWT technique specifications. If the OWT is not shut down during a strong seismic event, the excessive tilt of the tower will cause great damage to the rotating blades and gear system, seriously affecting the service life of the OWT. Therefore, it is recommended that seismic monitoring equipment should be installed on OWTs by the designer and manufacturer. Once the occurrence of a strong earthquake is perceived, the OWT should be immediately shut down through the servo control system, thus ensuring the safety and long-term service performance of the OWT and enhancing its seismic performance. In addition, the displacement response at Position 4 indicates that the high-frequency components of the incident seismic wave are absorbed by the loose seabed foundation soil. The presence of the seabed foundation has an extremely significant effect on the seismic dynamics of the OWT. The analysis results will have no credibility if the effect of seabed foundation is not taken into consideration in the seismic analysis of OWTs.

The distribution of horizontal displacement and bending moment along the height of the tower and monopile is illustrated in Fig. 9. It can be seen that the horizontal displacement of the tower increases non-linearly from the bottom to the top. The maximum displacement of the steel pile in the *x*-*y* plane is 2.6 m, and the corresponding inclination angle of the tower is about 1.4°. Actually, there is a very strict limitation on the inclination angle of the tower cylinder for the normal service of OWTs, e.g., DNVGL (2016) [53] specifies that the inclination angle of the tower cylinder of OWTs caused by the deformation under the installation and loading conditions can't exceed 0.5°. The Thornton Bank Offshore Wind Farm was designed adopting a standard that the tower cylinders didn't tilt more than 0.25° [54]. The national standard of China, i.e., Technical Standards for Wind Farm Engineering (FD 003–2007) [55], specifies that the allowable inclination angle of the tower cylinder of OWTs with a height over 100 m is only 0.17°. In this study, the maximum inclination angle of the tower is 1.4°, which has exceeded the limitation on the inclination angle for normal service. The OWT needs to be shut down for protection. Otherwise, the service life of this OWT will be seriously affected.

Fig. 9 (d) shows that the maximum bending moment in the turbine tower and monopile is about 30,000 kN•m, occurring near the static water level $z = 95$ m, which is also the connection part between the tower and the monopile. The maximum tensile and compressive stresses on the section (thin-walled circular ring) of the tower can be evaluated by Equation (1), according to the theory of Material Mechanics.

$$\sigma_{\max} = MR/I_y \tag{1}$$

where $\sigma_{\max}$ is the maximum tensile and compressive stresses, M is the maximum bending moment, R is the radius of the outer ring of the thin-

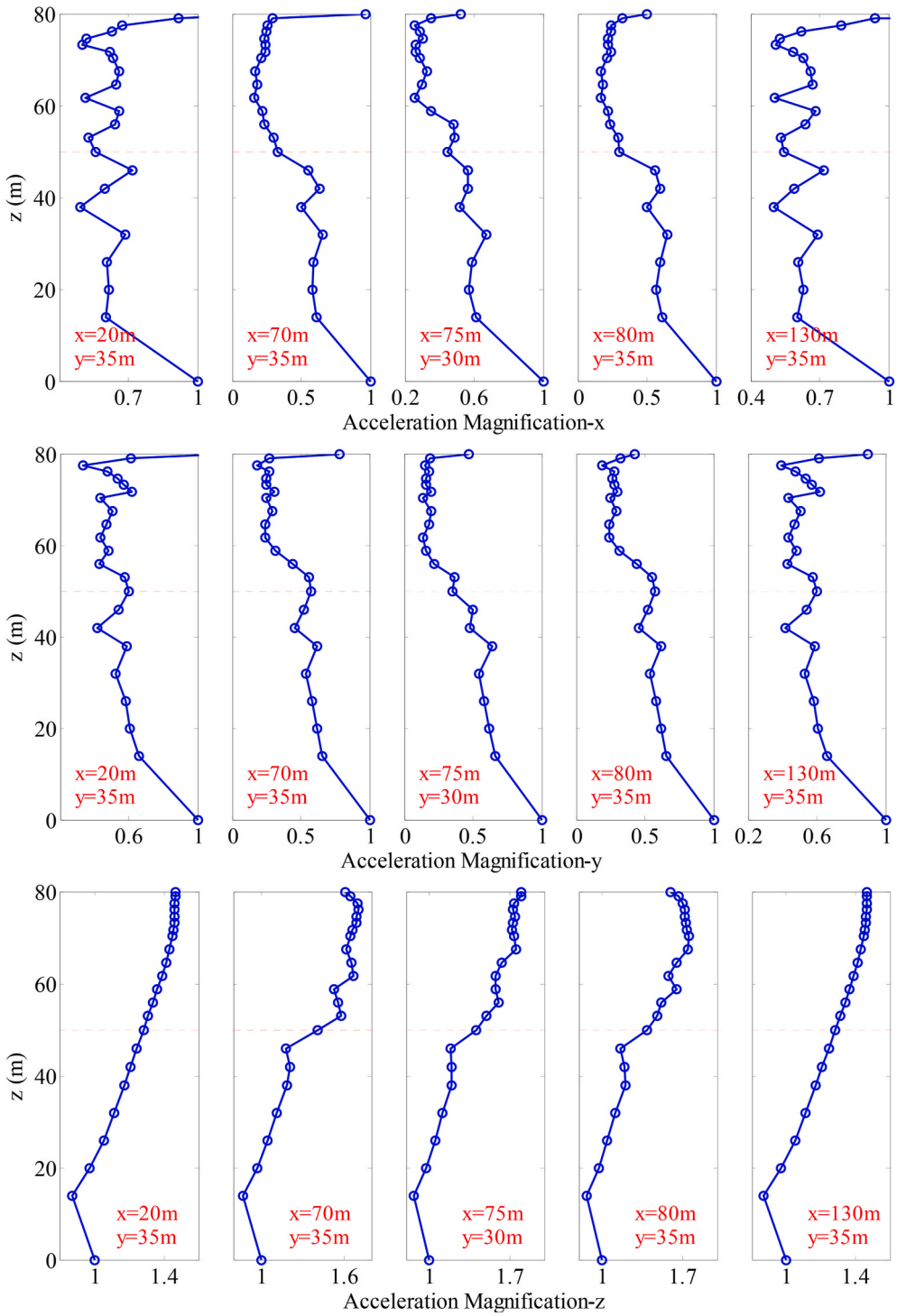

Fig. 12. Peak acceleration magnification along the height it locates in the seabed foundation relative to the input seismic wave at several typical positions.

walled monopile, and I_y is the moment of inertia of the ring section to the y-axis. It is calculated that the maximum stress on the cross-section of the tower is about $\sigma_{max} = 71$ Mpa. It is well known that Q345 steel is commonly used in the OWT manufacturing industry to manufacture the tower. Under normal temperatures, the yield stress of the steel monopile is at least 345 Mpa, which is 4.9 times the maximum stress inside the tower. It indicates that the turbine tower has enough structural safety performance and well fatigue resistance. The strength of the flange and bolts connecting the tower and the monopile needs to be paid more attention to ensure the seismic stability of OWT.

3.2.2. *Acceleration*

A comparison of the acceleration time histories at Positions 1 and 4 on the OWT with that at the bottom of the seabed foundation is shown in Fig. 10. It can be seen that the high-frequency components of the horizontal (x and y direction) seismic waves are absorbed and the low-frequency components are significantly amplified at Position 1. The amplitude of the horizontal acceleration at Position 4 is significantly less than that of the input seismic wave, which means considerable energy attenuation occurs in the horizontal direction as the seismic wave propagates within the seabed foundation. However, the absorption and amplification effects of the seabed foundation on seismic waves are not

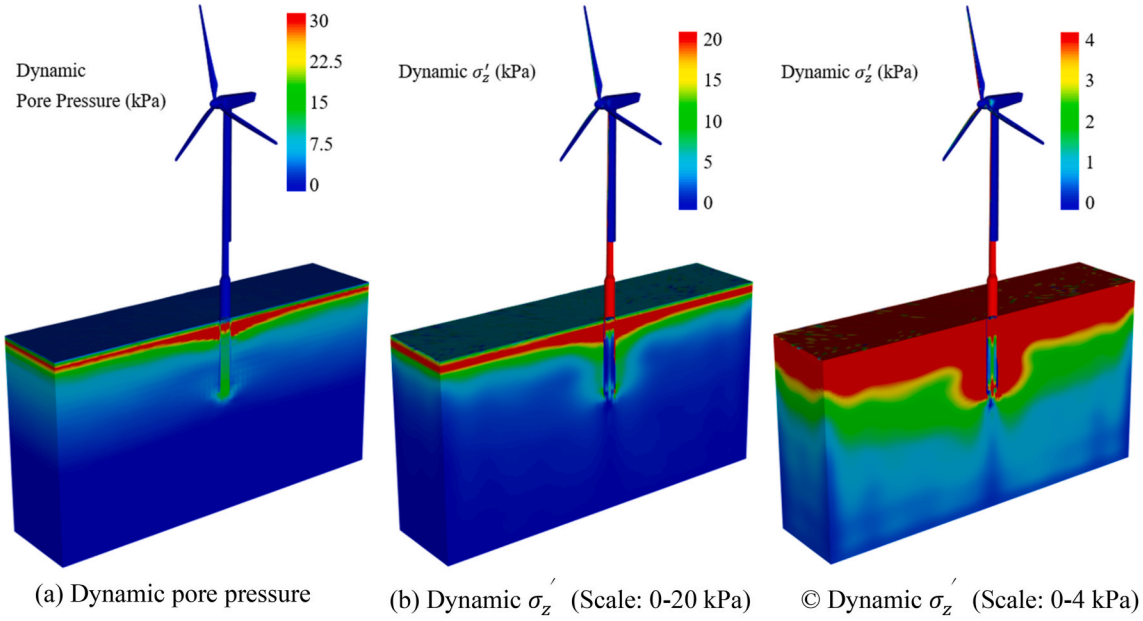

Fig. 13. Distribution of pore pressure and effective stress at $t = 300$ s (Noted: the initial values are excluded, and the seabed foundation is sectioned by $y = 35$ m).

significant in the vertical direction. Comparing the acceleration response at Positions 1 and 4, it can be found that the horizontal acceleration amplitude at Position 1 (at the top of the OWT) is about 6–8 times that at Position 4 (at the bottom of the monopile). It is indicated that the structure of OWT has a very significant amplification effect on the horizontal seismic wave, and the high-frequency components are almost filtered out completely. In the vertical direction, the structure of OWT also has an amplification effect on the seismic wave, but it is much less significant than that in the horizontal direction. In addition, the high-frequency components of the seismic wave are not filtered by the structure of OWT in the vertical.

The distribution of the amplification of peak acceleration along the tower and monopile is shown in Fig. 11. The distribution of the amplification of the peak acceleration along the height in the seabed foundation is shown in Fig. 12. It can be seen that the amplification to the peak acceleration in the three directions is roughly positively correlated with the height that it locates on the tower and monopile. However, within the seabed foundation, the peak acceleration amplification in the horizontal direction is negatively correlated with the height it locates, and it is roughly positively correlated with the height it locates in the vertical direction. This phenomenon further indicates that considerable energy attenuation occurs during the propagation of the horizontal seismic wave within the seabed foundation, while the energy absorption to the vertical seismic wave is not significant. This result is consistent with the results demonstrated in Fig. 10. The presence of the seabed foundation has a very significant effect on the dynamic response of the OWT, and the complex mechanical behavior of the seabed soil should be considered in the dynamic analysis of OWTs.

3.2.3. *Pore pressure and effective stress*

The distribution of seismic wave-induced dynamic pore pressure and effective stress in the seabed foundation at $t = 300$ s (At the end of seismic wave incidence) is shown in Fig. 13. Negative values of effective stress mean that the seabed soil is compressive, and positive values of dynamic effective stress mean that the effective stress has reduced. It can be seen that the pore pressure in the shallow layer of the seabed foundation has accumulated, and the effective stress has reduced under seismic action. Due to the short drainage path of the seabed superficial soil, the pore pressure in the seabed superficial soil is difficult to accumulate. Hence, the blue area in the superficial layer of the seabed foundation appears in Fig. 13 (a). Under the blue area, there is a region with a thickness of about 3–4 m in which the residual pore pressure reaches 30 kPa, and correspondingly the effective stress σ_z' decreases by about 20 kPa, as illustrated in Fig. 13 (b). It can also be seen in Fig. 13 (c) that the reduction of effective stress in the seabed soil surrounding the monopile is greater than that in the far field. This indicates that the presence of the monopile promotes the occurrence of softening and liquefaction of the seabed soil around it.

The time histories of pore pressure and effective stress at two typical positions in the seabed foundation around the monopile, A and B, are shown in Fig. 14. Position A is located at a shallow depth of 3 m in the seabed foundation ($z = 77$ m), and position B is located at the same elevation as the bottom of the monopile ($z = 50$ m). It can be seen that the pore pressure at position A keeps accumulating and building up, and the effective stress gradually reduces until it is close to 0, indicating that the seabed soil at position A is finally liquefied. The pore pressure at position B has also accumulated and the effective stress has decreased, but its vertical effective stress is finally still greater than 350 kPa, indicating that the seabed soil here is not liquefied at all. It can be inferred that the shallow seabed soils around the monopile have liquefied during this seismic event, while the deep seabed soils have not liquefied. The specific distribution of the liquefaction zone will be discussed in the next section.

3.2.4. *Liquefaction zone*

The seabed foundation is generally the soil layers that are newly and rapidly deposited in the Quaternary, which is broadly distributed worldwide, typically soft with a low bearing capacity, and prone to soften or liquefy under cyclic loading [56,59]. There are two criteria for the residual liquefaction of loose seabed soil. (1) Criterion based on pore pressure: when the residual pore pressure is greater than the initial effective stress, seabed soil is considered to be liquefied. However, Ye and Wang [47] found that the seabed soil below a breakwater didn't liquefy, even though the excess residual pore pressure is two times the initial effective stress. Owing to the intensive soil-structure interaction, the displacement of marine structures may cause the current effective stress somewhere inside the seabed foundation to be much greater than the initial effective stress. Therefore, the relationship between excessive residual pore pressure and initial effective stress is insufficient to judge whether the seabed soil is liquefied or not, with the existence of marine

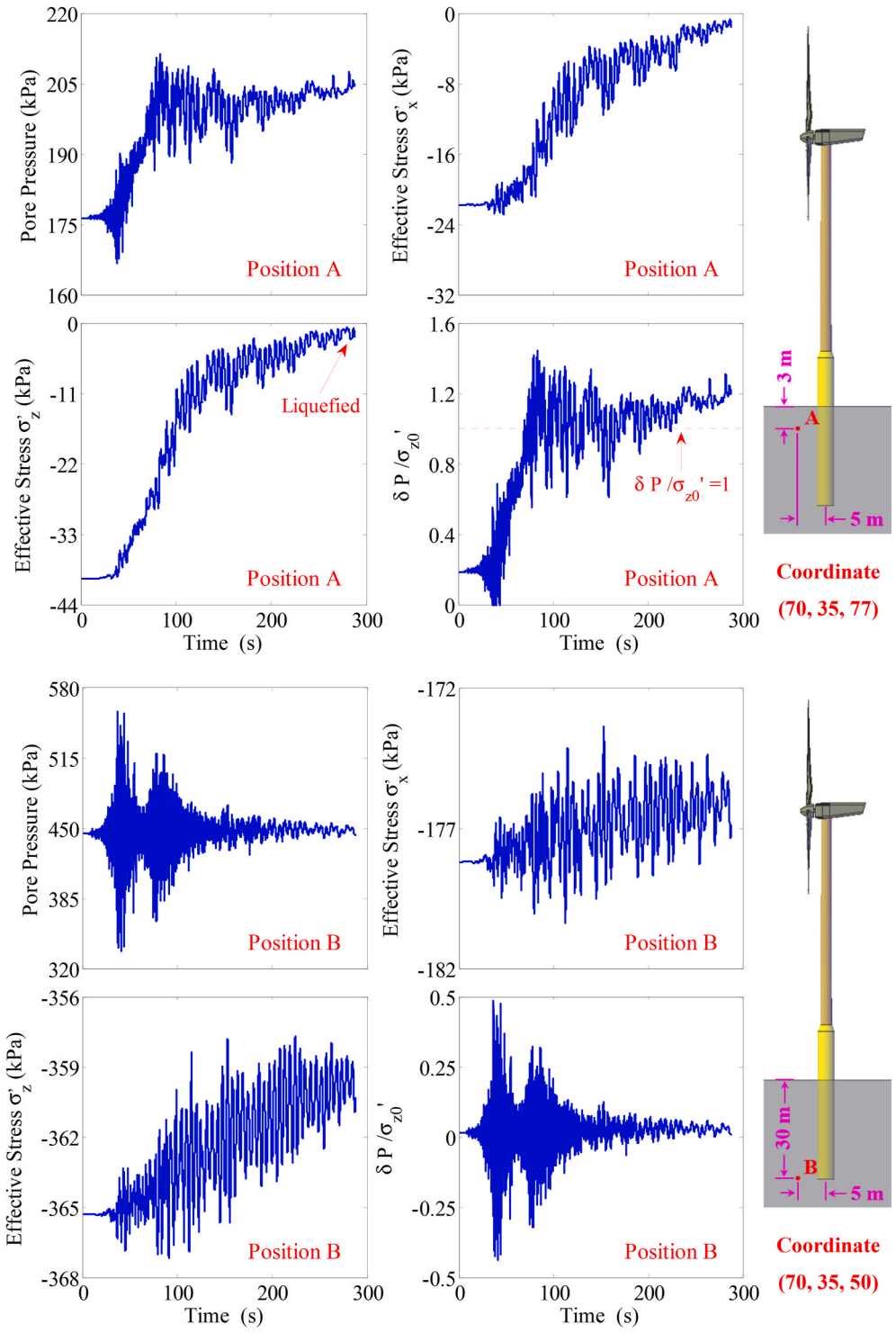

Fig. 14. Time histories of pore pressure and effective stress at position A and position B which are located inside the seabed near the monopile.

structures. (2) Criterion based on stress: when the current effective stress is close to or equal to 0, the seabed soil here is considered to be liquefied. Owing to the presence of cohesion, cohesive soil is more resistant to liquefaction than sandy soil. Based on this recognition, Yang and Ye [57] defined the liquefaction potential $L_{potential}$ to describe the possibility of liquefaction:

$$L_{\text{potential}} = \frac{\sigma'_{zd}}{-\sigma'_{z0} + \alpha c} \tag{2}$$

where $\sigma'_{zd} = \sigma'_z - \sigma'_{z0}$ is the vertical dynamic effective stress, σ'_z is the current vertical effective stress, σ'_{z0} is the initial vertical effective stress, c is the cohesion ($c = 0$ for sand), and α is a coefficient related to the material properties. Ye and Wang [47] provided a criterion for the liquefaction of loose seabed, i.e., the seabed soil is considered to be liquefied when $L_{\text{potential}} \geq 0.86$.

Since the liquefaction criterion based on pore pressure is not applicable to the presence of structures, the stress-based criterion is used in this study. The distribution of liquefaction zones in the seabed

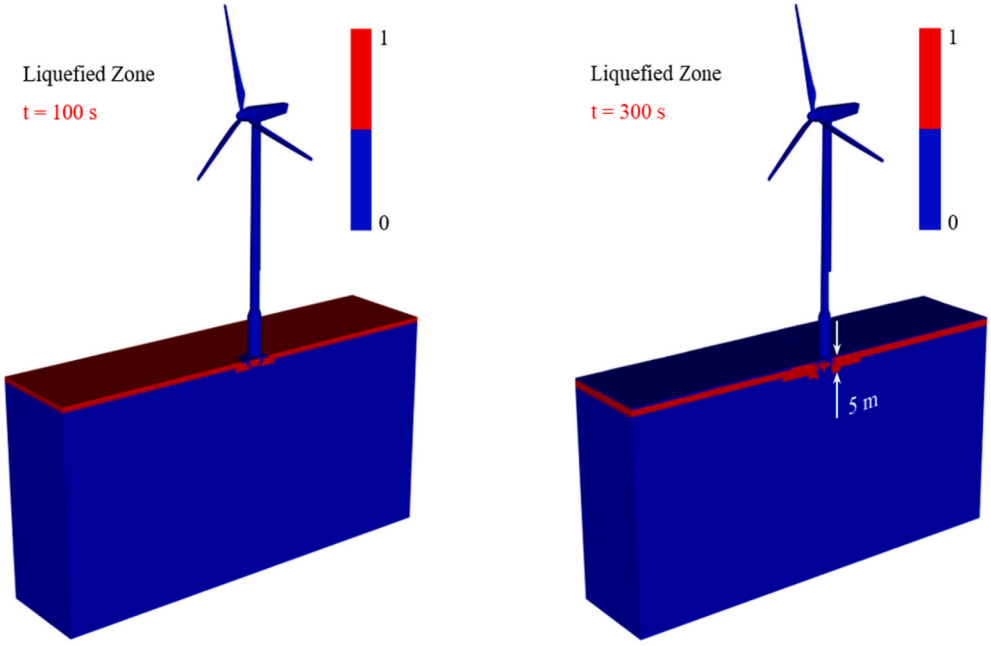

Fig. 15. Liquefaction zone (Red color) in the seabed foundation at $t = 100$ s and $t = 300$ s.

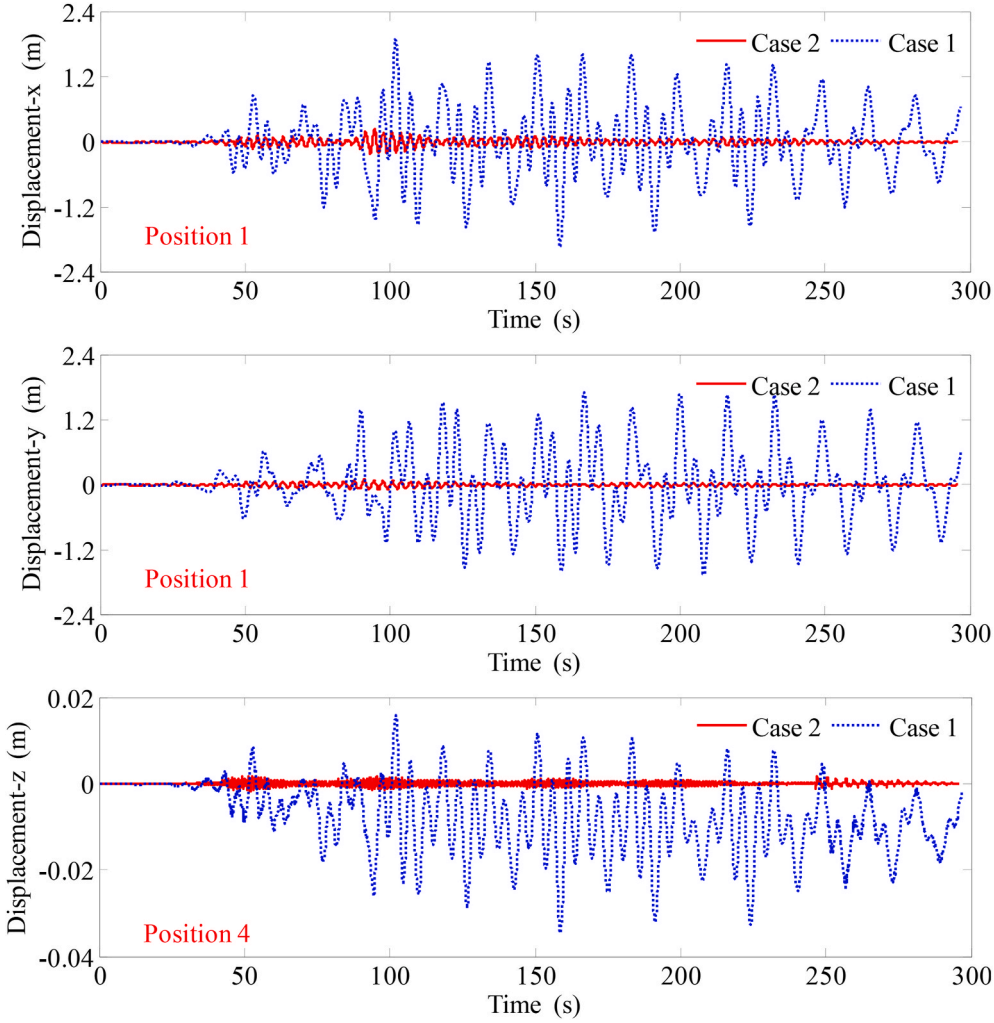

Fig. 16. Comparison of the time histories of the horizontal displacement at Position 1, and the settlement at Position 4 between Case 2 and Case 1.

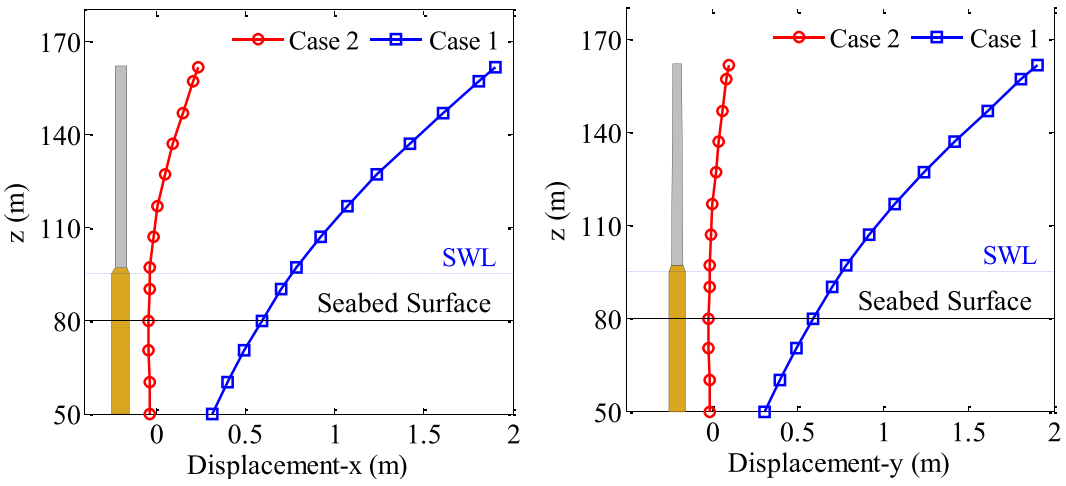

Fig. 17. Comparison of the peak horizontal displacement along the height of the OWT between Case 2 and Case 1.

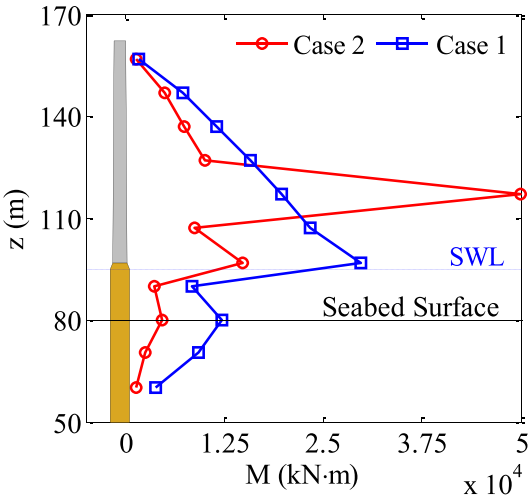

Fig. 18. Comparison of the maximum bending moment along the height of the OWT between Case 2 and Case 1.

foundation is shown in Fig. 15 (Noted: liquefaction zone is indicated by red color) at t = 100 s and 300 s. It can be seen that at t = 100 s, liquefaction occurs in the shallow layer of the seabed foundation, and the thickness of the liquefaction zone is 3–4 m. At t = 300 s, the superficial soil layer with a thickness of about 1 m of the seabed foundation turns from a liquefied state to a non-liquefied state. This is because the drainage path of the superficial layer of soil is short, and the previously accumulated pore pressure dissipates more rapidly. As a result, a non-liquefied layer is formed on the superficial layer of the seabed foundation. This phenomenon has also been discovered by Ye and Wang [58] already. One more important phenomenon that can be found in Fig. 15 is that the liquefaction zone within the seabed foundation surrounding the monopile is relatively large and the liquefaction depth reaches 5–6 m. This phenomenon indicates that the presence of the monopile enhances the seismic liquefaction depth in the seabed soil surrounding the monopile. Overall, the depth of the liquefaction zone is only 1/6 of the buried depth of the monopile, and the non-liquefied seabed soil could still provide sufficient lateral bearing capacity. This is the main reason why no horizontal residual displacement occurs for the OWT in this study. In order to fully guarantee the safety performance of an OWT, the lateral bearing capacity provided by the seabed soil within the liquefaction zone should not be considered in the seismic design.

4. Analysis of influencing factors

4.1. Effect of the complex behavior of seabed soil

Limited by the technical tools, the complex dynamic behaviors of the seabed soils (e.g., the accumulation of pore water pressure, the softening, and the liquefaction of soil) are generally omitted among the existing studies on the seismic dynamics of OWTs. Alternatively, seabed soil is often simplified as a rigid body or pore-elastic medium. In Case 2, the seabed soil is set as a poroelastic medium for the purpose of comparative study. The Young's modulus and Poisson's ratio of the seabed soil are 5.0 × 10^8 Pa and 0.30, respectively, while the other parameters in Case 2 are the same as that in Case 1. The effects of the complex mechanical behaviors of seabed soil can be investigated by taking the results of Cases 1 and 2.

The time histories of the displacement at the top and bottom of the tower (i.e., Position 1 and Position 4) in Case 1 and Case 2 are shown in Fig. 16, and the peak value of the horizontal displacement along the height of the tower and monopile is shown in Fig. 17. It can be seen that both the horizontal and vertical displacements in Case 2 are much less than that in Case 1.

The maximum bending moment along the height of the tower and the monopile between Case 1 and 2 are shown in Fig. 18. In case 2, the maximum bending moment along the tower is 50000 kN m, which is 1.7 times that in Case 1. It is indicated that if the complex mechanical behaviors of the seabed soil are not reasonably considered, and the seabed foundation is treated as a rigid body or a linear elastic material in numerical simulation, the deformation of the tower will be seriously underestimated and the bending moment in the tower will be overestimated. During the design of OWTs, it is generally necessary to increase the diameter or wall thickness of the tower to enhance its anti-bending performance. If the bending moment is overestimated, the design parameters of OWTs will be too conservative, which will cause unnecessary waste in finance.

The time histories of the seismic acceleration at Position 1 in both Case 1 and Case 2 are compared in Fig. 19. It can be seen that the high-frequency components are dominated in Case 2, while the low-frequency components dominate in Case 1. It is indicated that high-frequency components have not been absorbed or filtered during the propagating of the seismic wave in Case 2. The maximum vertical acceleration in Case 2 is 4.8 m/s^2, which is twice that in Case 1.

It can be indicated that the complex mechanical behavior of seabed soils play important role in the numerical simulation, and the seismic dynamics of OWTs cannot be precisely described if the plastic behavior is not reasonably considered. This simplification will cause a great deviation in the estimation of the displacement, bending moment in the

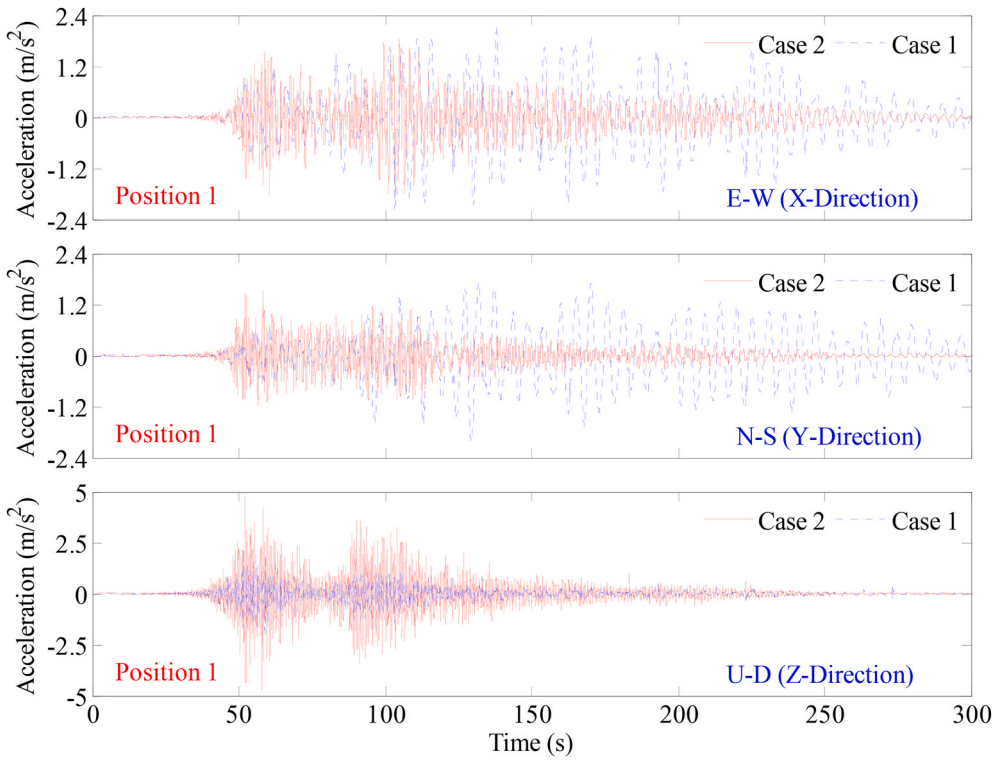

Fig. 19. Comparison of the time histories of the acceleration response at Position 1 between Case 2 and Case 1.

turbine tower, and the frequencies and amplitude of the acceleration response. As a result, it is difficult to make a reasonable evaluation of the stability of OWTs.

4.2. Effect of geometric shape and mass distribution of OWT

If considering the complex geometry shape of the OWT blades and nacelle, their FEM meshes are quite difficult to obtain. Thus, these OWT components with complex shapes were usually simplified into equivalent loads in the previous FEM simulations. In Case 3, the OWT is simplified as a thin-walled steel pipe with a thickness of 50 mm, and the blades and nacelle are replaced by a vertical loading according to the equivalence of their gravity force. The value of the equivalent vertical loading is 736 kN, which is determined according to the parameters listed in Table 1. In Case 3, the vertical loading is uniformly applied on the top of the tower. The effects of geometric shape and mass distribution of the OWT can be investigated by comparing the results from Case 1 and Case 3.

The time histories of the horizontal displacement at the top (i.e., where $z = 160$ m) and the vertical displacement at the bottom of the OWT tower (i.e., Position 4) are shown in Fig. 20. It can be seen that: (1) The frequencies of the seismic displacements in Cases 1 and 3 are close to each other, and the vertical settlement in these two cases is also close to each other. (2) The horizontal displacement at the top of the OWT tower in Case 3 is less than that in Case 1, which indicates the equivalent of the geometry shape and mass distribution will lead to the underestimation of the horizontal deformation of OWTs.

The maximum horizontal displacement along the height of the OWT tower and monopile is shown in Fig. 21. Generally speaking, the maximum horizontal displacement in Case 3 is less than that in Case 1. As for the monopile which is buried in the seabed foundation, the horizontal displacement in the two cases is close to each other. As the increasing of height, the deviation between them is getting greater. Due to the omitting of the inertial effect caused by the simplification in Case 3, the seismic displacements and tilting angle of the OWT are underestimated, which is unfavorable for the security of the OWT.

The time histories of the seismic acceleration at the top of the OWT tower (i.e., where $z = 160$m) in Cases 1 and 3 are shown in Fig. 22. It can be seen that: (1) The response of acceleration in Cases 1 and 3 are similar. In both cases, the high-frequency components of the horizontal seismic wave are absorbed, while the low-frequency components are amplified. (2). The maximum horizontal acceleration in Case 3 is generally greater than that in Case 1, which must be caused by the omitting of the mass inertia of the blades and nacelle in Case 3. In the vertical direction, the time histories of acceleration response in the two cases are basically the same.

The amplification factor for the horizontal seismic acceleration along the height of the OWT in Case 1 and 3 are shown in Fig. 23. Compared with Case 1, the amplification to the horizontal acceleration is greater while the amplification to vertical acceleration is less in Case 3.

The above results show that if the complex geometric shape, mass distribution, and mass inertia effect of the OWT are not considered, the displacement of the OWT tower will be underestimated, the acceleration response will be overestimated, and the inclination angle of the tower will be underestimated. The safety factor of the OWT which is obtained based on the equivalent loading method is overestimated, which will bring extra risk to the stability of OWTs. Therefore, the seismic stability evaluation for OWTs taking the equivalent loading method is defective.

4.3. Effect of hydrostatic pressure imposed on the monopile and seabed foundation

The hydrostatic pressure applied on the seabed surface and the lateral outer surface of the monopile is considered in Case 1 (i.e., SWL = 95m and $d = 15$m). In Case 4 (i.e., SWL = 80m, $d = 0$m), the static water level is considered the same as the seabed surface, and the hydrostatic pressure is omitted. Thus, the effect of the hydrostatic pressure of seawater on the seismic dynamics of the OWT can be investigated by comparing the results in Cases 1 and 4. It should be noted that during an earthquake event, the monopile of OWTs is affected not only by the hydrostatic pressure but also by the dynamic pressure induced by the earthquake vibration (i.e., hydrodynamic pressure). However, the effect

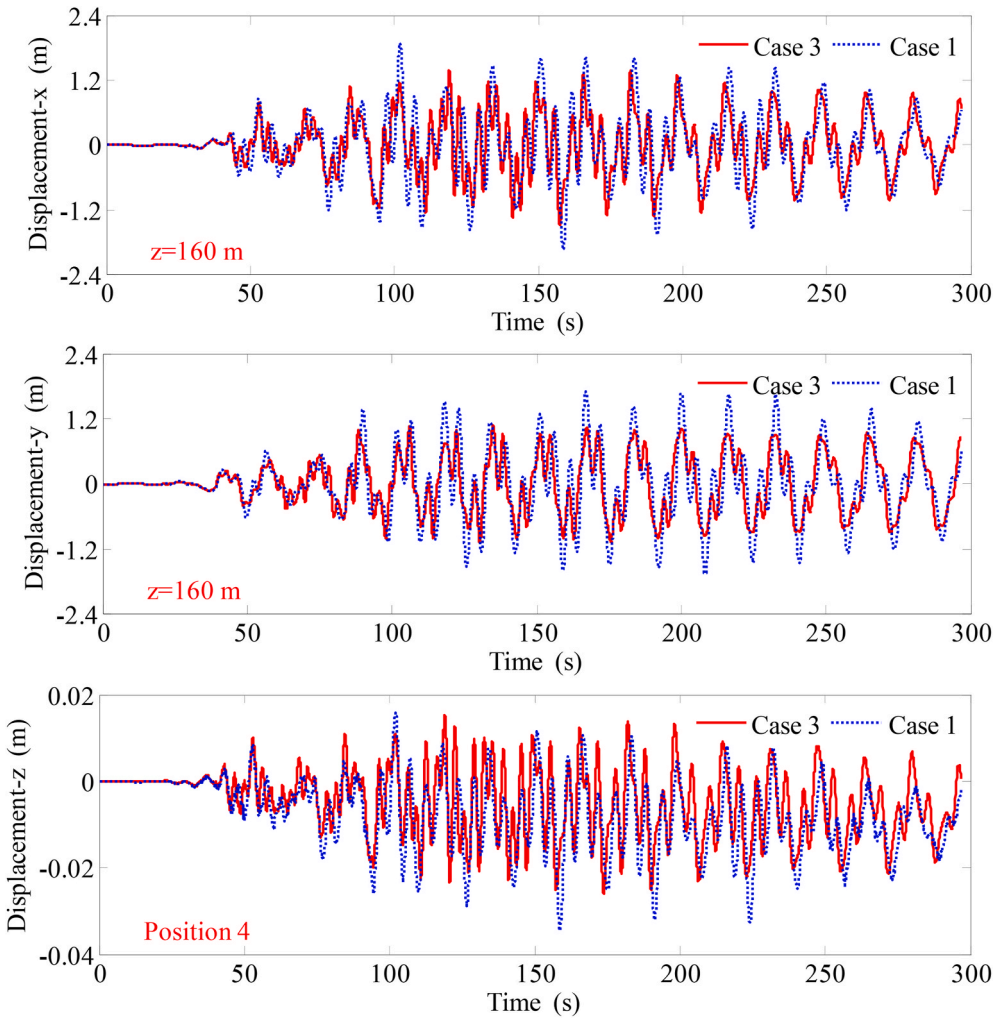

Fig. 20. Comparison of the time histories of the horizontal displacement at the top ($z = 160$ m), and the settlement at the bottom (Position 4) of the OWT between Case 3 and Case 1.

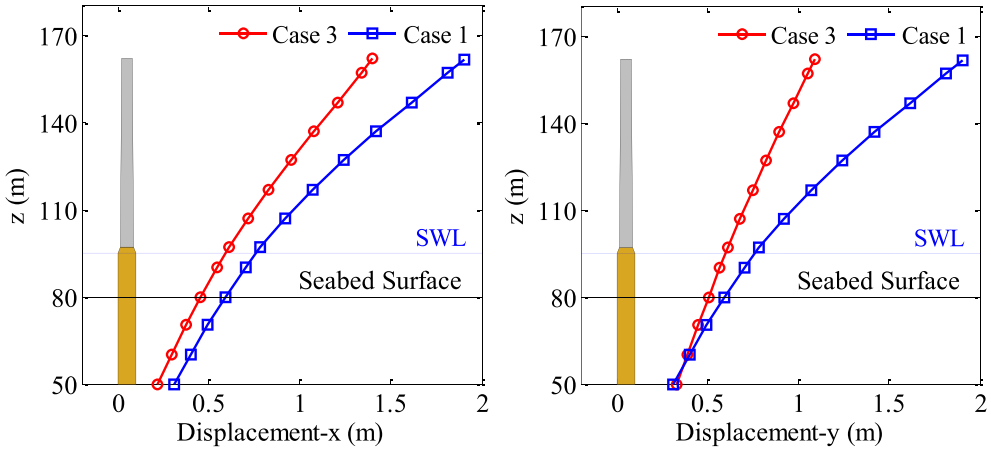

Fig. 21. Comparison of the peak horizontal displacement along the height of the OWT between Case 3 and Case 1.

of the hydrodynamic pressure on the seismic dynamics of OWTs is usually ignored in existing studies. Limited by technique tools, the effect of hydrodynamic pressure on the monopile is also omitted in this study, and such research would be carried out in the future.

The time histories of the horizontal displacement at Position 1 and the vertical displacement at Position 4 in Cases 1 and 4 are shown in Fig. 24. The time histories of the excess pore pressure and effective stress at Position A in Case 1 and Case 4 are shown in Fig. 25. It can be seen that the displacement, excess pore pressure, and effective stress in Case 1 and Case 4 are almost similar to each other. Thus, it can be indicated that the effect of hydrostatic pressure on the seismic dynamics of the seabed foundation and OWT is quite marginal and can be reasonably ignored in

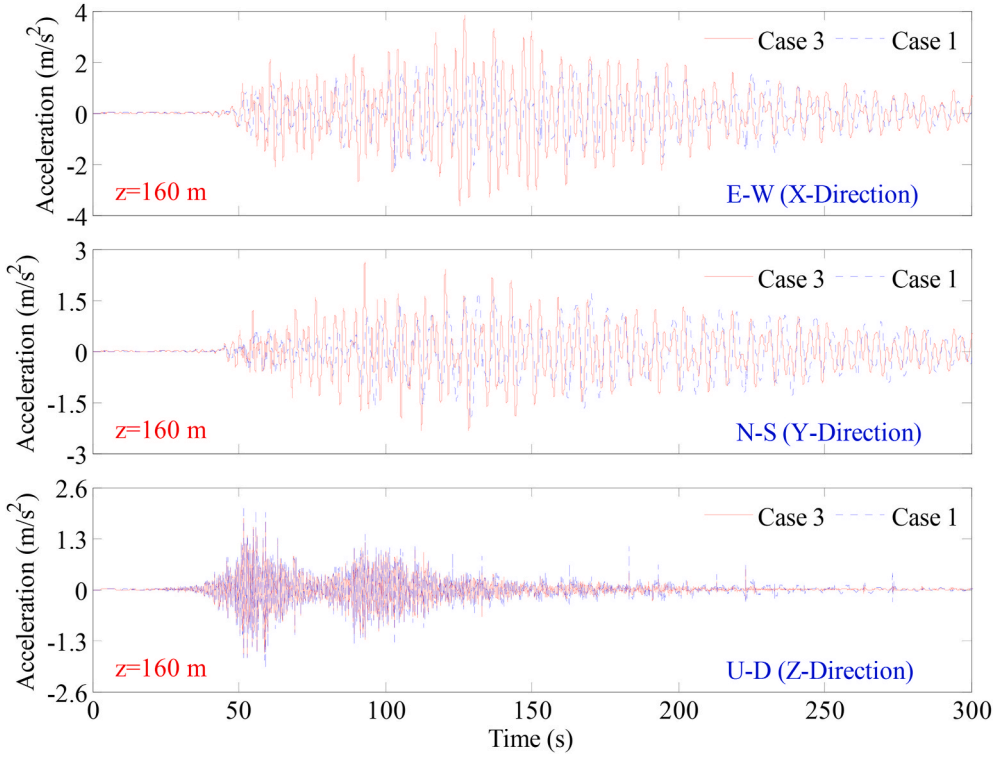

Fig. 22. Comparison of the time histories of the acceleration at $z = 160$m between Case 3 and Case 1.

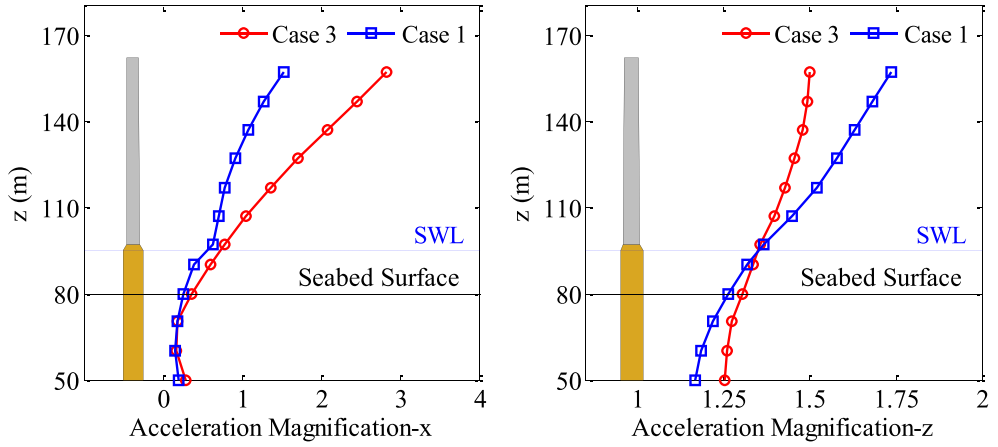

Fig. 23. Comparison of the peak acceleration amplification along the height of the OWT between Case 3 and Case 1.

numerical simulation.

4.4. *Effect of pore water inside seabed foundation*

The seismic dynamics of OWTs actually has been previously explored by adopting the 'Soil Model' module of ABAQUS in the existing references, in which the pore water was not considered. Furthermore, the term of acceleration in Biot's equation was not considered in this commercial software. Thus, the seismic dynamics of saturated soil can't be modeled by ABAQUS, strictly speaking. In other words, the existence of pore water can't be taken into account in the seismic dynamics analysis of OWTs. It is noted that real seabed soils are typical water-saturated materials, and the strong nonlinearity caused by the interaction between pore water, soil skeleton, and the structures of OWTs can't be ignored. In Case 5, the seabed foundation is treated as a one-phase material and the existence of pore water is not considered. Thus, the effects of pore water inside the seabed foundation can be investigated by comparing the results in Case 1 and Case 5.

The time histories of the horizontal displacement at Position 1 in Cases 1 and 5 are shown in Fig. 26. It can be seen that: (1) The maximum horizontal displacement in Case 5 is slightly greater than that in Case 1, which mainly contributes to the decaying effects of the interaction between the pore water and soil skeleton in Case 1 on the seismic displacement. (2) The predominant periods in Case 5 are slightly greater than in Case 1, which is also affected by the pore water-soil skeleton interaction. Moreover, the cyclic softening or liquefaction induced by the accumulation of excess pore water pressure will change the stiffness of the seabed foundation, making the basic natural frequencies of the seabed-OWT system correspondingly change. Thus, the effect of pore water on the modal characteristic of the OWT should be considered in engineering design. However, there are few works that focus on this topic at present and it needs further studies.

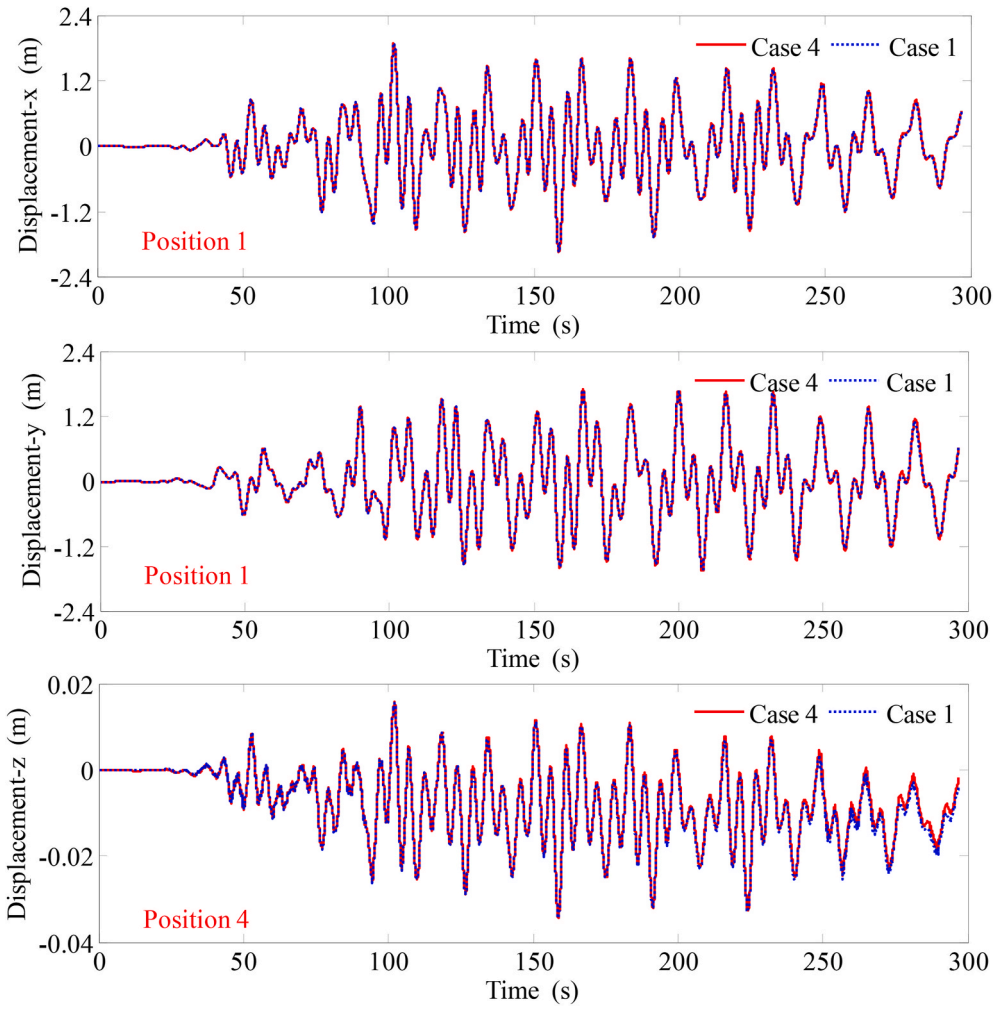

Fig. 24. Comparison of the time histories of the horizontal displacement at the top ($z = 160$ m) and the settlement at Position 4 between Case 4 and Case 1.

The amplification factors of the seismic acceleration along the height of the OWT in Case 1 and Case 5 are shown in Fig. 27. It can be seen that compared with Case1, the OWT has a greater magnification to the horizontal acceleration and a smaller magnification to the vertical acceleration in Case 5. The time histories of the effective stress at Position A within the seabed foundation are shown in Fig. 28. It can be seen that the effective stress in Case 5 only fluctuates and has no reduction occurring, which is of cause caused by the omitting of the pore water.

The above results show the seismic analysis of the OWT is incredible if the existence of pore water inside the seabed foundation is not taken into consideration, because the accumulation of excess pore pressure and cyclic softening of soil can't be captured.

5. Conclusion

In this study, FssiCAS, which is a marine geotechnics numerical software, is adopted as the computational platform, the seismic dynamics of a 1.5 MW OWT and its seabed foundation are comprehensively and systematically studied, and the stability of the OWT is further evaluated. Here, the complex mechanical behavior of the seabed foundation is described utilizing the generalized elastoplastic soil model PZIII, and the complex geometry and mass distribution of OWT are taken into account in computation by the way of precisely modeling and meshing the blades and nacelle. Besides, four comparative cases are designed to study the effects of four major factors on the seismic response of the OWT and its seabed foundation. Based on the computational results, the following recognitions are obtained.

(1) Under strong seismic waves, the OWT and its seabed foundation have a strong dynamic response, such as the substantial shaking of the OWT, the accumulation of pore pressure, and reduction of effective stresses, as well as liquefaction within the seabed foundation. In the cases involved in this study, the center of the turbine blades has a shaking amplitude of 2 m in the horizontal direction under the incident peak acceleration of 0.1g. However, the OWT doesn't produce residual displacement and still had quite well seismic stability, indicating that the liquefaction occurring in the superficial layer of the seabed foundation does not necessarily affect the stability of OWTs. In seismic design, engineers need to credibly assess the depth of the liquefaction zone under the fortified seismic condition. It should be noted that the lateral bearing capacity of the seabed soils within the depth of liquefaction can't be used.

(2) Due to the pile-soil interaction, the liquefaction depth of the seabed soil surrounding the monopile is significantly greater than that at the far field, i.e., the monopile promotes the liquefaction in the seabed soil surrounding it.

(3) The maximum bending moment in the turbine tower in this study is about 30000 kN•m, which occurs at the connection part between the tower and the monopile. The tower has sufficient strength to avoid yielding damage. In the seismic design of OWTs, it is necessary to pay attention to the strength of the flanges and bolts which connect the tower and the monopile.

(4) There is great energy attenuation during the propagation of seismic waves within the seabed foundation. Most of the high-

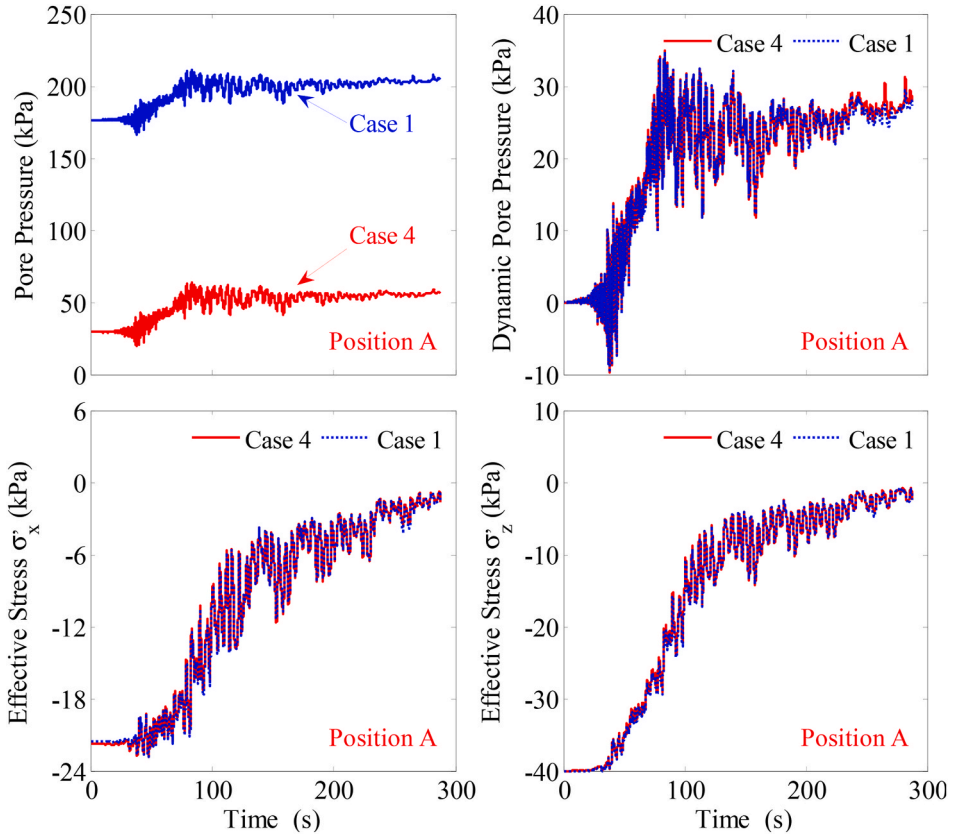

Fig. 25. Comparison of the time histories of the pore pressure and effective stress at Position A between Case 4 and Case 1.

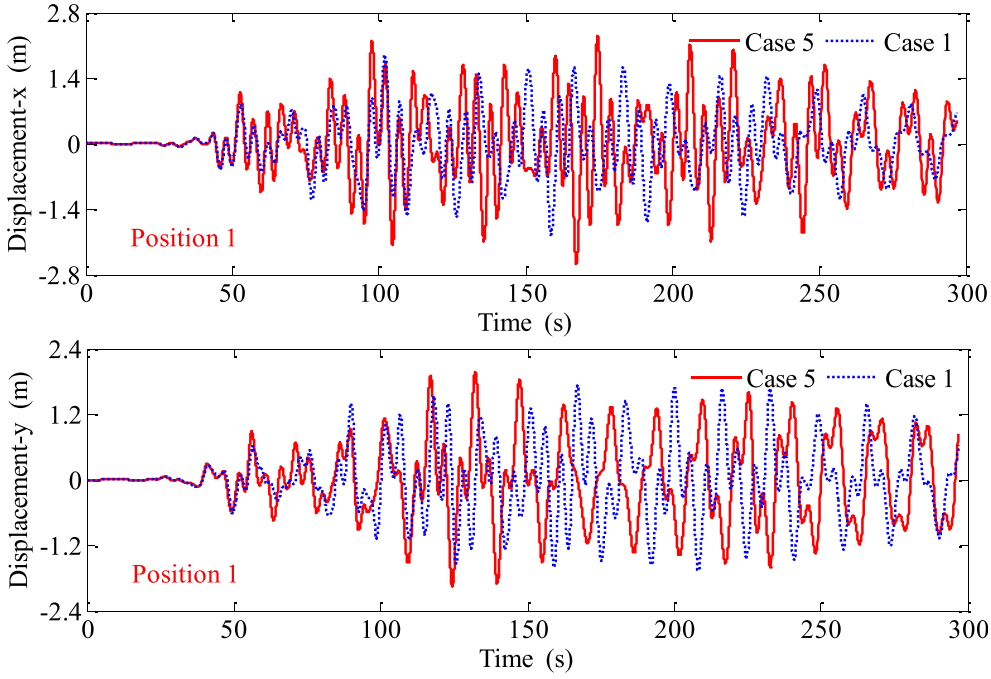

Fig. 26. Comparison of the time histories of the horizontal displacement at Position 1 between Case 5 and Case 1.

frequency components are absorbed by the seabed soil, and some of the low-frequency components are amplified. The amplification of the horizontal peak acceleration is negatively correlated with the height it locates on the tower, while the vertical peak acceleration amplification is positively correlated with height.

(5) When the complex mechanical behavior of the seabed foundation soil is not considered and the seabed foundation is treated as a rigid body or a porous linear elastic material, the displacement of the OWT will be underestimated, and the bending moment inside the turbine tower will be overestimated, which in turn will lead to

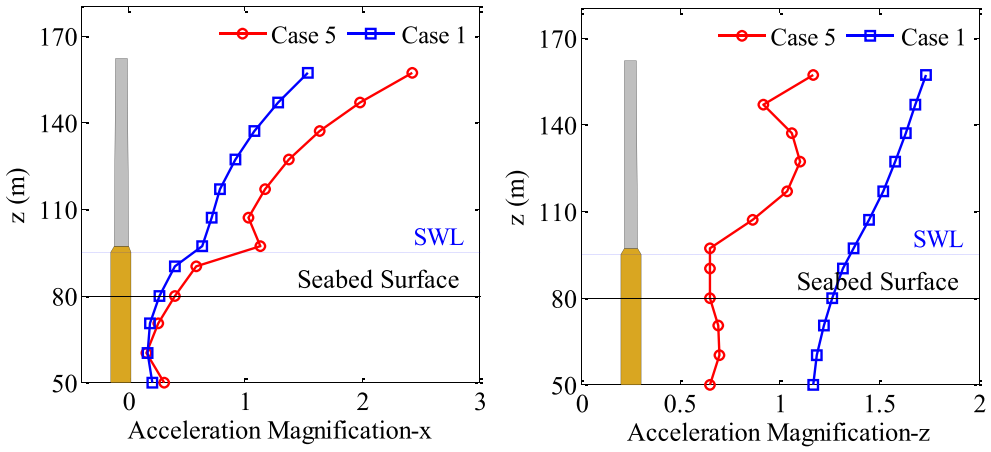

Fig. 27. Comparison of the peak acceleration amplification along the height of the OWT between Case 5 and Case 1.

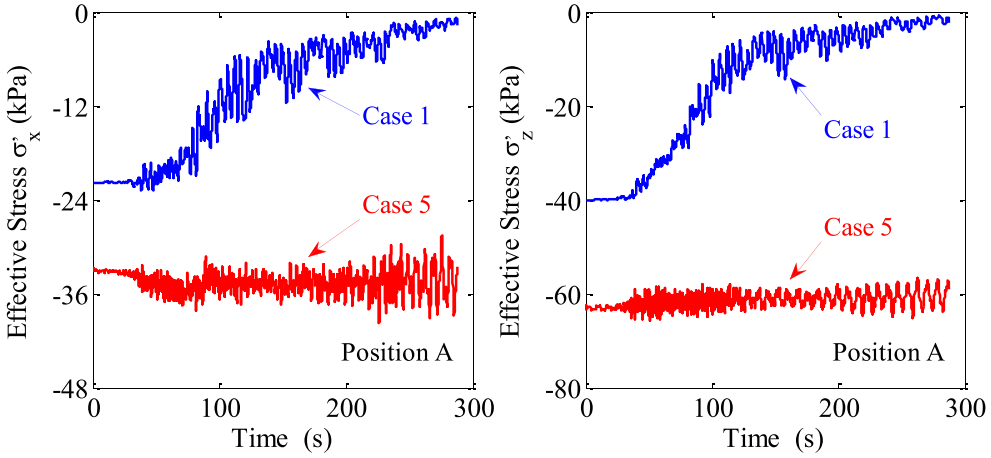

Fig. 28. Comparison of the time histories of the effective stress at position A between Case 5 and Case 1.

some overly conservative design parameters for the moment of inertia for the tower section.

(6) When the complex geometry and mass distribution of the OWT are not considered, and the equivalent load is used to equivalently replace the gravity effect of the turbine blades and nacelle, the displacement and the inclination of the OWT will be underestimated, and the safety factor will be overestimated. These may bring certain risks to the long-term service life of the OWT.

(7) The hydrostatic pressure of seawater has no effect on the seismic response of OWTs and seabed foundations.

(8) When the presence of pore water within the seabed foundation is not considered, the analysis of the dynamic response characteristics and inherent natural frequencies of the whole OWT-seabed foundation system is not credible, as the softening and liquefaction behavior of seabed soils can't be captured.

(9) The equipped capacity of OWTs currently in use is generally 8–10 MW, with the highest being up to 16 MW in China. Although the OWT involved in this study is not large in size, the above knowledge obtained in this study should be equally applicable to larger OWTs.

Declaration of competing interest

The authors declare that they have no known competing financial interests or personal relationships that could have appeared to influence the work reported in this paper.

Data availability

Data will be made available on request.

Acknowledgments

This work is grateful for the funding support from the National Natural Science Foundation of China, Grant No. 51879257.

References

[1] E. Vanem, T. Fazeres-Ferradosa, A truncated, translated Weibull distribution for shallow water sea states[J], Coast. Eng. 172 (2022), 104077.
[2] M.A. Asareh, W. Schonberg, J. Volz, Effects of seismic and aerodynamic load interaction on structural dynamic response of multi-megawatt utility scale horizontal axis wind turbines, Renew. Energy 86 (2016) 49–58.
[3] I. Prowell, An Experimental and Numerical Study of Wind Turbine Seismic Behavior, Dissertations & Theses - Gradworks, 2011.
[4] X.Y. Zheng, H. Li, W. Rong, et al., Joint earthquake and wave action on the monopile wind turbine foundation: an experimental study, Mar. Struct. 44 (2015) 125–141.
[5] X. Wang, X. Zeng, X. Yang, J. Li, Seismic response of offshore wind turbine with hybrid monopile foundation based on centrifuge modelling, Appl. Energy 235 (2019) 1335–1350.
[6] X. Wang, X. Zeng, X. Li, J. Li, Liquefaction characteristics of offshore wind turbine with hybrid monopile foundation via centrifuge modelling, Renew. Energy 145 (2020) 2358–2372.
[7] X. Li, X. Zeng, X. Yu, et al., Seismic response of a novel hybrid foundation for offshore wind turbine by geotechnical centrifuge modeling, Renew. Energy 172 (2021) 1404–1416.

[8] C. Ji, J. Zhang, Q. Zhang, et al., Experimental investigation of local scour around a new pile-group foundation for offshore wind turbines in bi-directional current, China Ocean Eng. 32 (6) (2018) 737–745.
[9] E. Zhao, B. Shi, K. Qu, et al., Experimental and numerical investigation of local scour around submarine piggyback pipeline under steady current, J. Ocean Univ. China 17 (2) (2018) 244–256.
[10] Z. Gao, N. Saha, T. Moan, et al., Dynamic analysis of offshore fixed wind turbines under wind and wave loads using alternative computer codes, in: Proceedings of the 3rd Conference on the Science of Making Torque from Wind, June., 2010, pp. 28–30.
[11] Y. Guanche, R. Guanche, P. Camus, et al., A multivariate approach to estimate design loads for offshore wind turbines, Wind Energy 16 (7) (2013) 1091–1106.
[12] Y. Yang, C. Li, M. Bashir, et al., Investigation on the sensitivity of flexible foundation models of an offshore wind turbine under earthquake loadings, Eng. Struct. 183 (2019) 756–769.
[13] Y. Yang, M. Bashir, C. Li, et al., Mitigation of coupled wind-wave-earthquake responses of a 10 MW fixed-bottom offshore wind turbine, Renew. Energy 157 (2020) 1171–1184.
[14] H. Zuo, K. Bi, H. Hao, et al., Influence of earthquake ground motion modelling on the dynamic responses of offshore wind turbines, Soil Dynam. Earthq. Eng. 121 (2019) 151–167.
[15] H. Matlock, Correlation for design of laterally loaded piles in soft clay, in: Offshore Technology Conference, OnePetro, 1970.
[16] M. Huang, J. Yu, C. Zhang, p–y curves of laterally loaded piles in clay based on strain path approach, 03, Chin. J. Geotech. Eng. 37 (2015) 400–409 (In Chinese).
[17] J. Häfele, C. Hübler, C.G. Gebhardt, et al., An improved two-step soil-structure interaction modeling method for dynamical analyses of offshore wind turbines, Appl. Ocean Res. 55 (2016) 141–150.
[18] F. Taddei, M. Schauer, L. Meinerzhagen, A practical soil-structure interaction model for a wind turbine subjected to seismic loads and emergency shutdown, Procedia Eng. 199 (2017) 2433–2438.
[19] V.L. Krathe, A.M. Kaynia, Implementation of a non-linear foundation model for soil-structure interaction analysis of offshore wind turbines in FAST, Wind Energy 20 (4) (2017) 695–712.
[20] Y.Y. Ko, A simplified structural model for monopile-supported offshore wind turbines with tapered towers, Renew. Energy 156 (2020) 777–790.
[21] K.A. Abhinav, N. Saha, Stochastic response of jacket supported offshore wind turbines for varying soil parameters, Renew. Energy 101 (2017) 550–564.
[22] H. Zuo, K. Bi, H. Hao, Dynamic analyses of operating offshore wind turbines including soil-structure interaction, Eng. Struct. 157 (2018) 42–62.
[23] J. Domínguez, R. Gallego, B.R. Japón, Effects of porous sediments on seismic response of concrete gravity dams, J. Eng. Mech. 123 (4) (1997) 302–311.
[24] P. Wang, M. Zhao, X. Du, et al., Wind, wave and earthquake responses of offshore wind turbine on monopile foundation in clay, Soil Dynam. Earthq. Eng. 113 (2018) 47–57.
[25] X. Wang, X. Zeng, X. Yang, et al., Seismic response of offshore wind turbine with hybrid monopile foundation based on centrifuge modelling, Appl. Energy 235 (2019) 1335–1350.
[26] A. Ali, R. De Risi, A. Sextos, et al., Seismic vulnerability of offshore wind turbines to pulse and non-pulse records, Earthq. Eng. Struct. Dynam. 49 (1) (2020) 24–50.
[27] L.J. Prendergast, K. Gavin, P. Doherty, An investigation into the effect of scour on the natural frequency of an offshore wind turbine, Ocean Eng. 101 (2015) 1–11.
[28] H. Ma, J. Yang, L. Chen, Effect of scour on the structural response of an offshore wind turbine supported on tripod foundation, Appl. Ocean Res. 73 (2018) 179–189.
[29] K. Meng, C. Cui, Z. Liang, et al., A new approach for longitudinal vibration of a large-diameter floating pipe pile in visco-elastic soil considering the three-dimensional wave effects[J], Comput. Geotech. 128 (2020), 103840.
[30] C. Cui, K. Meng, C. Xu, et al., Vertical vibration of a floating pile considering the incomplete bonding effect of the pile-soil interface[J], Comput. Geotech. 150 (2022), 104894.
[31] C. Cui, Z. Liang, C. Xu, et al., Analytical solution for horizontal vibration of end-bearing single pile in radially heterogeneous saturated soil[J], Appl. Math. Model. 116 (2023) 65–83.
[32] L. Wang, Y. Zhang, Influence of Simplified Models on Seismic Response Analysis of Wind Turbine Towers. Applied Mechanics and Materials, vol. 94, Trans Tech Publications Ltd, 2011, pp. 369–374.
[33] Y. Yan, Y. Yang, M. Bashir, et al., Dynamic Analysis of 10 MW Offshore Wind Turbines with Different Support Structures Subjected to Earthquake Loadings, Renewable Energy, 2022.
[34] Handbook of Seismic Risk Analysis and Management of Civil Infrastructure systems [M], Elsevier, 2013.
[35] I. Anastasopoulos, M. Theofilou, Hybrid foundation for offshore wind turbines: environmental and seismic loading, Soil Dynam. Earthq. Eng. 80 (2016) 192–209.
[36] R. Xi, X. Du, P. Wang, et al., Dynamic analysis of 10 MW monopile supported offshore wind turbine based on fully coupled model, Ocean Eng. 234 (2021), 109346.
[37] R. Mo, R. Cao, M. Liu, et al., Seismic fragility analysis of monopile offshore wind turbines considering ground motion directionality, Ocean Eng. 235 (2021), 109414.
[38] S. Zhang, J. Zhang, Y. Ma, et al., Vertical dynamic interactions of poroelastic soils and embedded piles considering the effects of pile-soil radial deformations, Soils Found. 61 (1) (2021) 16–34.
[39] Y. Zhang, C. Liao, J. Chen, et al., Numerical analysis of interaction between seabed and mono-pile subjected to dynamic wave loadings considering the pile rocking effect, Ocean Eng. 155 (2018) 173–188.
[40] Z. Lin, D. Pokrajac, Y. Guo, et al., Investigation of nonlinear wave-induced seabed response around mono-pile foundation, Coast. Eng. 121 (2017) 197–211.
[41] L. Wang, J. Zhang, R. Cai, et al., Wave effects on the anti-liquefaction of the seabed around composite bucket foundation of offshore wind turbines, J. Hydrodyn. 33 (6) (2021) 1291–1302.
[42] Y. Yang, M. Bashir, C. Li, et al., Mitigation of coupled wind-wave-earthquake responses of a 10 MW fixed-bottom offshore wind turbine, Renew. Energy 157 (2020) 1171–1184.
[43] M.A. Asareh, I. Prowell, J. Volz, et al., A computational platform for considering the effects of aerodynamic and seismic load combination for utility scale horizontal axis wind turbines, Earthq. Eng. Eng. Vib. 15 (1) (2016) 91–102.
[44] D.S. Jeng, J.H. Ye, J.S. Zhang, et al., An integrated model for the wave-induced seabed response around marine structures: model verifications and applications, Coast. Eng. 72 (2013) 1–19.
[45] J. Ye, D. Jeng, R. Wang, et al., A 3-D semi-coupled numerical model for fluid–structures–seabed-interaction (FSSI-CAS 3D): model and verification, J. Fluid Struct. 40 (2013) 148–162.
[46] K. He, T. Huang, J. Ye, Stability analysis of a composite breakwater at Yantai port, China: an application of FSSI-CAS-2D, Ocean Eng. 168 (2018) 95–107.
[47] J. Ye, G. Wang, Seismic Dynamics of Offshore Breakwater on Liquefiable Seabed Foundation, Soil Dynamics and Earthquake Engineering, 2015.
[48] M. Pastor, O.C. Zienkiewicz, A.H.C. Chan, Generalized plasticity and the modelling of soil behavior, Int. J. Numer. Anal. Methods GeoMech. 14 (3) (1990) 151–190.
[49] J. Ye, K. He, Dynamics of a pipeline buried in loosely deposited seabed to nonlinear wave & current, Ocean Eng. 232 (2021), 109127.
[50] O.C. Zienkiewicz, A.H.C. Chan, M. Pastor, et al., Computational geomechanics[M], Wiley, Chichester, 1999.
[51] S. Jung, S.R. Kim, A. Patil, Effect of monopile foundation modeling on the structural response of a 5-MW offshore wind turbine tower, Ocean Eng. 109 (2015) 479–488.
[52] J.H. Ye, D.S. Jeng, Three-dimensional dynamic transient response of a poro-elastic unsaturated seabed and a rubble mound breakwater due to seismic loading, Soil Dynam. Earthq. Eng. 44 (2013) 14–26.
[53] G.L. Dnv, Dnvgl-Rp-C203, Fatigue Design of Offshore Steel Structures, DNV GL, Oslo, Norway, 2016.
[54] K. Peire, H. Nonneman, E. Bosschem, Gravity base foundations for the thornton bank offshore wind farm, Terra Aqua (Engl. Ed.) 115 (115) (2009) 19–29.
[55] Fd 003-2007, Design Regulations on Subgrade and Foundation for WTGS of Wind Power station[S], China Water & Power Press, Beijing, 2007 (In Chinese).
[56] S. Sassa, T. Takayama, M. Mizutani, et al., Field observations of the build-up and dissipation of residual pore water pressures in seabed sands under the passage of storm waves, J. Coast Res. 39 (SpecialIssue) (2006) 410–414.
[57] G. Yang, J. Ye, Wave & current-induced progressive liquefaction in loosely deposited seabed, Ocean Eng. 142 (2017) 303–314.
[58] J. Ye, G. Wang, Numerical simulation of the seismic liquefaction mechanism in an offshore loosely deposited seabed, Bull. Eng. Geol. Environ. 75 (3) (2016) 1183–1197.
[59] K.P. He, J.H. Ye, Dynamics of offshore wind turbine-seabed foundation under hydrodynamic and aerodynamic loads: a coupled numerical way, Renew. Energy 202 (2023) 453–469, 2023.